Nanomechanics of Single Biomacromolecules

33

Qing Li, Zackary N. Scholl, and Piotr E. Marszalek

Keywords
Atomic force microscopy • Force spectroscopy • Nanomaterials • Nanomechanics • Protein folding • Single molecules

Introduction

Biopolymers such as nucleic acids, proteins, and polysaccharides play diverse biological functions and are components of various materials. Nucleic acids encode hereditary information and instructions for protein synthesis. In addition, the unique hybridization properties of nucleic acids provide building blocks of nanomaterials, nanomachines, and nanosensors [1–13] and are considered as a viable platform for highly parallel biological computing [14–18]. Proteins mainly perform enzymatic reactions and participate in cellular signal transduction and communication but also play critical structural and mechanical roles (e.g., supporting cell shape and elasticity) and are natural components of bioadhesives, biocomposites [19, 20], and bio-fibers like collagen [21] and silk [22–24]. Natural, synthetic, and hybrid proteins have recently been exploited for development of new biomaterials with rationally tuned elastic properties [25–29]. Polysaccharides, either alone or as components of glycoproteins or peptidoglycans that are exploited for energy storage, participate in molecular recognition between biomolecules and also play important structural roles, e.g., in the cell wall of plants and

These authors contributed equally to this work

Q. Li (✉) • P.E. Marszalek
Department of Mechanical Engineering and Materials Science, Center for Biologically Inspired Materials and Material Systems, and Duke University, Durham, NC, USA
e-mail: ql24@duke.edu; pemar@duke.edu

Z.N. Scholl
Program in Computational Biology and Bioinformatics, Duke University, Durham, NC, USA
e-mail: zns@duke.edu

B. Bhushan et al. (eds.), *Handbook of Nanomaterials Properties*,
DOI 10.1007/978-3-642-31107-9_13,

bacteria and as components of hydrogels and biofilms [30, 31]. They are also components of many natural and semisynthetic materials (e.g., paper, cotton, rayon).

The mechanical properties of individual biomacromolecules and their nanostructures are critically important for their biological and other functions. For example, the mechanics of the DNA double helix plays an important role during cell division, DNA replication, DNA damage repair, and transcription of DNA information onto RNA [32]. The mechanics of protein networks, such as present in the extracellular matrix, is essential for cell shape, cell flexibility, and binding interactions between cells (cell adhesion) [33–70]. Also, muscle elasticity is partially determined and regulated by the elastic properties of giant modular proteins [71–76]. The mechanics of polysaccharide chains (such as cellulose chains and fibers) is important in providing rigidity to cellular structures (e.g., wood), and the flexibility of sugar rings is exploited in molecular recognition between sugars and lectins and is important for enzymatic reactions such as glycolysis [77]. The combined mechanics of proteins and polysaccharides is exploited in biohydrogels such as those lubricating joints [78–81]. Since these biomacromolecules are also used as building blocks for various nanostructures and nanomachines, the characterization of their mechanical properties is of considerable significance to nanotechnology. The progress in directly measuring mechanical properties of individual biomacromolecules paralleled the development of a variety of single-molecule visualization, manipulation, and characterization techniques. This chapter will briefly introduce the most popular single-molecule manipulation techniques and will review the nanomechanical properties of individual biomacromolecules determined using these methods.

Polymer Elasticity and Techniques to Study the Mechanical Properties of Single Polymer Molecules

The mechanical properties of individual biomacromolecules are typically examined by means of single-molecule force spectroscopy (SMFS) techniques [73, 82–89]. In SMFS, individual macromolecules or their fragments are attached to a substrate and to a force probe and stretched (by separating the two), and their extension and tension are accurately measured [90]. The relationship between the applied force (tension) and extension that describes molecule's elasticity has been coined a force spectrogram. Biomacromolecules covered in this chapter are polymeric in nature so they are composed of many identical or similar units (monomers). For this reason, the primary source of their elasticity is entropic in origin [91–94]. The entropy is at its maximum in equilibrium and is gradually decreased when the polymer ends are separated and the monomers are forced to align with the direction of the stretching force. Fully stretched polymers would have just a single configuration so their configurational entropy would be zero and attaining such a state would require an infinite force [94, 95]. However, even before such high forces are generated entropically, the chemical and physical bonds within the polymeric structure gradually extend according to their own stiffness and the polymer exhibits the

enthalpic elasticity that results in continually increasing the contour length of the polymer (overstretching) [73, 96]. The enthalpic elasticity may also manifest itself as an abrupt transition in the force–extension relationship typically in the form of a force peak or a force plateau, when individual bonds or their groups undergo a discrete conformational force-induced transition that results in an abrupt lengthening of the polymer [73, 83, 96–99].

Atomic Force Microscopy (AFM)

Advantages: Excellent length resolution, low-high force range (5–10,000 pN), and constant-velocity or constant-force conditions are available, no need for specialized attachment.

Disadvantages: Cantilever spring constants are difficult to determine accurately [100, 101], not suitable for probing events at low forces (<5 pN).

AFM was invented in 1986 by Binning, Quate, and Gerber [102, 103] on the basis of an earlier invention of the scanning tunneling microscope (STM) [104, 105]. AFM was initially applied primarily as an imaging tool, but soon its power for mechanical manipulation of individual biomolecules was realized [106]. In SMFS measurements by AFM, molecules are attached at their termini or at random positions to a substrate and to the AFM tip, either specifically through chemical bonds or using ligand–receptor specificity (e.g., avidin–biotin) or even nonspecifically through physisorption [90]. The molecules that formed a bridge between substrate and the tip may be stretched in solution, which is of significance to measurements on biomacromolecules. The stretching process is controlled by means of a highly precise piezoelectric actuator that moves the sample away from the AFM tip or vice versa. The force experienced by the molecule (its tension) is determined through monitoring the bending of the AFM cantilever, which is followed by a split photodiode that measures the position of a laser beam reflected off of the cantilever and projected onto the diode. Force and length resolutions of SMFS measurements by AFM are on the order of 1 pN and < 1 nm. The main advantages of AFM as a force spectrometer are its superb length resolution, the ability to stretch short molecules, and the ability to apply small forces (piconewton order) and uniquely also very large forces (tens of nanonewtons). Also, AFM force spectrometers are fast and allow large loading rates (force/time) that are of importance when studying lifetimes of intermolecular bonds. SMFS by AFM are typically carried out under constant extension rate [73] or force clamp conditions [107].

Optical Tweezers

Advantages: Excellent force resolution and excellent length resolution at low forces (0.1–100 pN).

Disadvantages: Requires functionalized biopolymers to tether to bead

Optical tweezers [108–111] use a focused laser light to create a potential well that traps dielectric objects, as first observed by A. Ashkin in 1970 [112]. An appropriately surface-functionalized micron-size dielectric bead (e.g., coated with avidin) can be used to attach to it a terminally functionalized biopolymer (e.g., biotin-labeled DNA) and can be captured by an optical trap. The other end of the

molecule can be attached to a surface or to another bead kept, e.g., in a glass pipette by suction. The molecule is stretched by moving the surface or the second bead away from the optical trap (e.g., by means of piezoelectric actuator). A microscope-based video system accurately monitors the position of the first bead relative to the center of the optical trap to determine the applied force, while the translation of the second bead is accurately measured to determine the molecule extension. Optical tweezers provide superb force and length resolution on the order of <0.1 pN and <1 nm and are widely used in SMFS of DNA and proteins.

Magnetic Tweezers

Advantages: Excellent force resolution at low and medium forces (0.01–100 pN), simple method for applying torque

Disadvantages: Requires functionalized biopolymers to tether to bead

Magnetic tweezers use micron-size superparamagnetic beads, which develop a net magnetic moment in an external magnetic field and are pulled by a magnetic force that is proportional to the field gradient [113–115]. Similar to optical tweezers, a molecule of interest can be tethered between a surface (bead) and a superparamagnetic bead and stretched by an external magnetic field. Forces on the order of 0.01–100 pN can be easily exerted by magnetic tweezers [94]. In addition to stretching, magnetic tweezers provide a very simple means to apply a torque to the molecule of interest allowing it to be rotated and coiled [113, 116–118].

Biomembrane Force Probe

Advantages: High precision in spring constant measurement, excellent force range (0.01–1,000 pN)

Disadvantages: Limited to probing molecules that appear on (or are introduced to) the cell surface

In the biomembrane force probe assay (BFP), a small glassy bead is biochemically "glued" to a pressurized membrane capsule (e.g., red blood cell membrane) that is held by a pipette through a controlled amount of suction [41]. Different negative pressures result in different membrane tension, so the probe stiffness can be easily controlled (by the pressure) and forces on the order of 0.01–1,000 pN can be generated. The bead itself is decorated at low surface density with molecules of interest that are brought to contact to their cognate receptors, presented on another cell. By forming contacts between the bead and the surface of the investigated cell, specific bonds between ligands (presented on the bead) and receptor (presented on the cell surface) are formed and then ruptured by moving the bead away from the cell surface. In this way bonds' strength and lifetimes can be accurately measured. Forces and extensions are determined via optical microscopy by the amount of deformation of the membrane transducer and the position of the glassy bead. Typical resolution is <0.5 pN and <5 nm [41, 119].

Nanopore Techniques

Advantages: Capabilities to uniquely measure size and charge of molecules

Disadvantages: Method not fully developed

Molecules pass through a nanometer-size pore in a membrane separating two compartments to which a potential gradient is applied and transiently block the ionic current flowing through the pore producing characteristic current blockage fingerprints. These current patterns can be used to infer various molecular properties of the traversing molecules, such as size and charge. It was proposed that natural or solid-state nanopores could be used to sequence long DNA strands, because characteristic blockage currents are different for different nucleobases [120–122]. Electric field-driven passage of charged biomacromolecules such as nucleic acids or uncharged but terminally functionalized with a charged "leader" (e.g., a short piece of DNA) molecules such as proteins can also be used to examine mechanical properties of traversing molecules. This is because in most cases these molecules are too bulky to pass through the pore and need to be stretched and unfolded before they will fit into a narrow pore [123, 124]. For direct measurements of the force applied to a molecule traversing a nanopore, its end can be attached a bead whose position can be accurately monitored in a force measuring optical trap [122].

Flow Techniques

Advantages: Readily simulate physiological flow conditions

Disadvantages: Requires careful calibration of flow to determine forces

Mechanical properties of biomacromolecules can also be studied by stretching them in an elongational flow [125, 126]. This can be achieved either directly due to the coupling of the flowing fluid with the molecule of interest or indirectly by attaching one end of the molecule to a surface and the other to a micron-size bead which then experiences a hydrodynamic force [127]. Also, to limit unwanted interactions between the molecule and the surface during flow measurements, a magnetic bead attached to the molecule of interest can be levitated magnetically while subjected to a horizontal hydrodynamic force [128].

Particle Tether

Advantage: Simple, inexpensive system suitable to various microscopy methods. The system does not involve external forces.

Disadvantage: Low spatial resolution

The tethered particle motion experiments (TPM) were first started by Jeff Gelles and colleagues in the early 1990s to study transcription by single RNA polymerase molecule [129, 130]. This method has been used to study DNA looping [131–142], DNA transposition [143], promoter sequences bending [144], and site-specific recombination [145, 146]. In a typical tethered particle experiment, a single polymer molecule is tethered between the microscope coverslip surface and a microsphere through specific binding [147]. Brownian motion of the bead is restricted to a semispherical region by the tethered polymer molecule and can be captured by an optical microscopy. Variance in travelling scope of the particle gives information about change in the length of the tethered polymer. TPM has the advantage of simple implementation, easy combination with optical and magnetic tweezers, and straightforward data analysis methods. However, TPM has low time

resolution caused by the time cost by the probe to explore the region limited by the polymer tether [148]. Attempts to improve the accuracy of TPM include investigation of the volume effects of the bead [149, 150], suppression of the Brownian motion of the bead [151], simultaneous tracing of hundreds of single molecules by biochip [152], and development of proper data analysis approaches to obtain reliable kinetic parameters from TPM measurements [148, 153, 154].

A detailed comparison of these various single-molecule manipulation techniques along with the description of their advantages and limitations can be found in a number of review articles [155–159].

Applications

In its force measuring mode, AFM is typically used to stretch and relax DNA, proteins, and sugars either in isolation or also on living cells [83, 86, 87, 160] to study their elasticity, mechanical, unfolding, refolding, and binding behaviors. At low forces (<20 pN) AFM force spectra capture the characteristic highly nonlinear entropic elasticity of biomacromolecules. At higher forces various deviations from the purely entropic elasticity are frequently observed [82]. These deviations are indicative of structural and conformational transitions induced by force that on the experimental time scale are either reversible or irreversible. For example, using AFM-based SMFS the elasticity of individual titin molecules that govern the passive elasticity of muscle was characterized in various force regimes [73]. It was found that the entropic alignment of titin immunoglobulin and fibronectin-type domains occurs at low stretching forces, and at higher forces, these domains reversibly unfold providing an extra length to the muscle when needed [75]. In addition AFM is frequently used to probe the strength of the interactions between various biomolecules including receptors and ligands pairs [43, 60, 161]. Optical tweezers are frequently used to examine the elasticity of biopolymers at low forces, and OT measurements can be set up to exploit the nanomechanical properties of biomacromolecules (such as DNA) [96] to study the mechanochemical behaviors of various enzymes that process these molecules (e.g., DNA and RNA polymerases) [162]. OT measurements can also be used to follow near equilibrium folding/unfolding behavior of proteins, either alone [163] or while interacting with ligands [164]. Magnetic tweezers found many applications to study torsional elastic properties of DNA and to follow the work of special DNA enzymes that affect coiling properties of DNA (such as gyrases) [165, 166]. BFP techniques were found particularly suited for measuring receptor–ligand interactions on live cells [167]. Nanopore techniques are used to study folding properties of biomacromolecules and to examine the interactions between various biomolecules, and they are continuously improved for DNA sequencing applications [122, 123, 168]. Flow techniques are used for biopolymer elasticity measurements and in conjunction with fluorescence video microscopy are being applied to follow the interactions between various biomacromolecules (e.g., DNA–protein interactions) [128].

Atomic Force Microscopy (AFM)

AFM Instrumentation

The schematic of an AFM instrument is shown in Fig. 33.1.

The principle of the AFM is conceptually simple: a small cantilever is first calibrated and then deflection of the cantilever during the stretching of an attached molecule is measured to precisely determine forces (from one to thousands of piconewtons) using Hooke's law. Cantilever deflection is measured and recorded by tracking voltage signal output from multi-segment photodiode detector (quadrant detector module in most recent design). The final signal used to convert to force recording is

$$V = \Delta V_{BT}/\Sigma$$

where ΔV_{BT} is the voltage difference between top and bottom area of the photodiode and Σ is the voltage sum from both areas. V is usually multiplied by an operational amplifier to improve the signal to noise ratio. The position of the sample is accurately controlled by a piezo actuator via a feedback–control loop with 0.2–0.5 nm resolution. These piezo actuator stages are usually equipped with

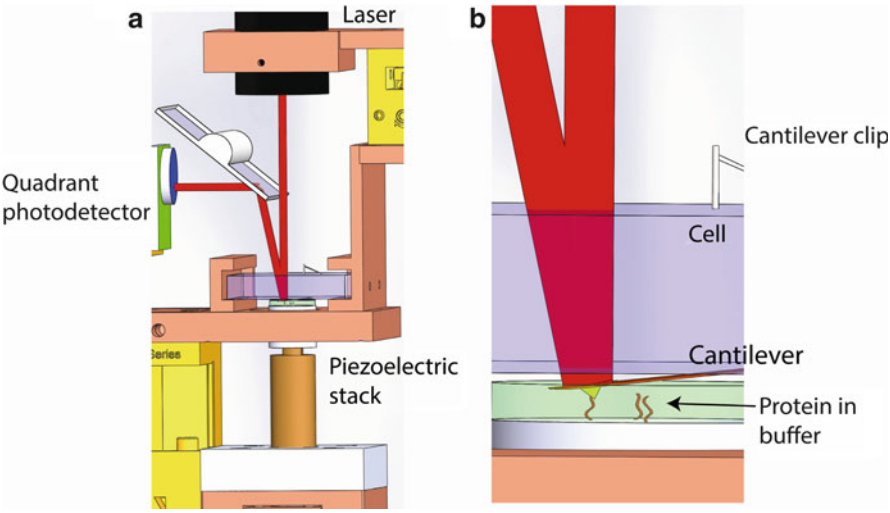

Fig. 33.1 (**a**) Schematic of an AFM instrument and (**b**) closeup of the cell containing the cantilever and probing the substrate. A laser probes the cantilever deflection which is detected using the difference between the top and bottom of a quadrant photodetector. The cantilever is suspended in a quartz cell over a substrate (clean glass or freshly evaporated gold) that has a drop of solution with the molecule of interest. A piezoelectric stack on the bottom controls the 3D movement of the substrate to contact the cantilever and then move away at constant force or constant velocity. Nonspecific attachment will allow the molecule (*red lines*) to attach to the cantilever and stretch the molecule of interest

capacitive or strain-gauge position sensors. The sensor signal output from the piezo controller is converted into distance using the voltage constant of the piezo,

$$\Delta z = C\Delta V$$

where C is the constant measured and given by piezo actuator factory specifications, Δz is the movement of the piezo, and ΔV is the sensor voltage signal output of the piezo actuator.

Cantilever calibration is based on thermal noise method (one of dynamic deflection methods proposed by Hutter and Bechhoefer [169]). In this method, the cantilever and the tip are treated together as a simple harmonic oscillator with one degree of freedom. Thermal fluctuations are considered as the only motion of the oscillator with the Hamiltonian

$$H = \frac{p^2}{2m} + \frac{1}{2}k_c q^2.$$

According to the equipartition theorem,

$$< \frac{1}{2}k_c q^2 > = \frac{1}{2}k_B T$$

where k_B is the Boltzmann's constant, k_C is the spring constant of the oscillator, T is the absolute temperature, and q is the displacement of the oscillator. Therefore, k_C can be obtained by measuring the mean-square spring displacement $< q^2 >$ due to thermal fluctuations at room temperature. This measurement is performed in the frequency domain by taking the power spectral density of the fluctuations of the photodiode signal δV (Fig. 33.2 is a representative power spectrum).

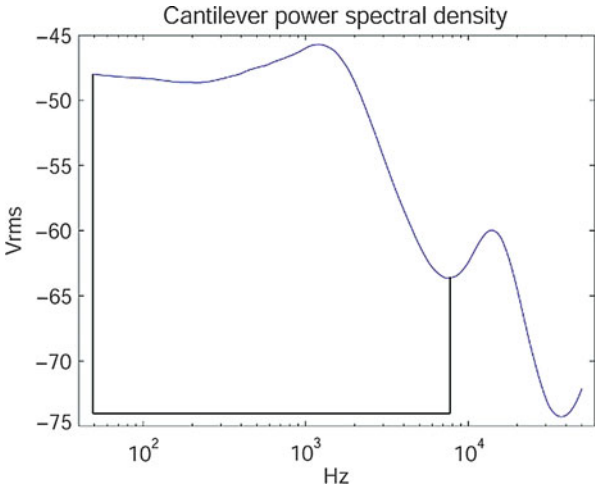

Fig. 33.2 A typical power spectral density curve of the photodiode signal thermal fluctuations. Frequencies are shown in their natural logarithm (dB) and signals are displayed in Vrms. Integration interval is between the *black lines*

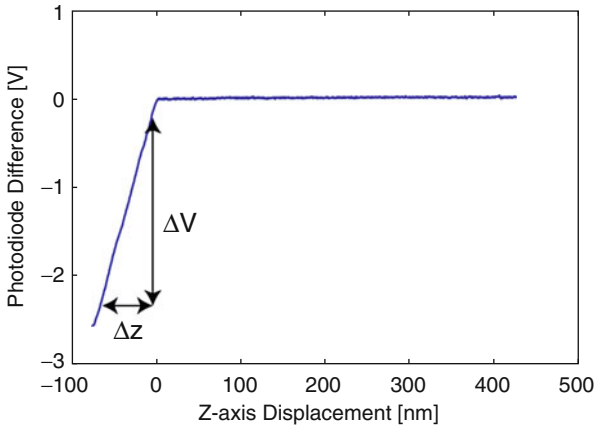

Fig. 33.3 Force spectrum. Voltage difference ΔV and piezo movement Δz used for slope calculation are shown in the graph

The integration is performed according to Parseval's equality

$$< \delta V^2 > = \frac{\int_a^b \delta V^2(t)dt}{\int_a^b dt} = \frac{\int_{a'}^{b'} FT^2(\delta V)df}{ENBW}$$

where FT(δV) is the Fourier transform of δV and ENBW is the equivalent noise bandwidth of the spectrum. Integration of the power spectrum is usually done in an interval close to the resonance frequency of the cantilever such as depicted in Fig. 33.2.

To finally convert the photodiode voltage signal into force, a force spectrum is acquired by moving the sample vertically using the piezo, while the position of the piezo and resulting cantilever deflection are recorded simultaneously (Fig. 33.3).

Then the slope of the deflection versus piezo position is

$$\text{slope} = \Delta z / \Delta V$$

Thus, the voltage signal from the photodiode, V, is interpreted to force by the following formula

$$F = k_c * V * \text{slope} = \frac{k_B T}{< \delta V^2 > * \text{slope}^2} * V * \text{slope}$$

where T is room temperature (usually 300 K).

Sample Preparation

The sample is prepared simply by depositing the molecule of interest in the relevant substrate. Substrates commonly used for AFM single-molecule force spectroscopy experiments are gold or glass. In the most basic experiment, molecules attach to the surface and the tip nonspecifically. Since the attachment is nonspecific, the location that the molecule absorbs to the tip and substrate is random. To circumvent the random attachment, there have been methods developed to control attachment to the surface and tip, like thiol chemistry [170], HaloTag7 immobilization [171], Strep-Tag immobilization [172], and Ni–NTA functionalization [173]. In any kind of immobilization, it is important to have a positive control to differentiate between single- and multimolecular AFM stretching experiments. Generally, only about 1 % of the data is usable. For protein unfolding experiments, a positive control can be designed by flanking the unknown protein of interest by previously characterized protein with known properties so that their presence indicates the recording is of a single molecule of interest (e.g., flanking unknown proteins by I27 domains of titin, which have a characteristic unfolding force of ~200 pN and a contour length increment of ~28 nm).

Stock solutions containing biomacromolecule (i.e., DNA, protein, polysaccharide) are usually diluted to 10–1,000 nM and incubated on the substrate for a period of time ranging from a few minutes to overnight. Appropriate incubation time and substrate choice are empirical and the ideal incubation case would allow the formation of a monolayer of the molecule on the substrate. Usually proteins are incubated on gold or functionalized glass for half an hour, DNAs are incubated on gold for more than 4 h, and polysaccharides are incubated on glass overnight. After incubation, the samples are usually washed several times before used for AFM pulling experiments to remove excess molecules that are not tethered to the surface of the substrates.

Experimental Procedure

AFM pulling experiments are carried out by gently moving the substrate relative to the cantilever tip through voltage applied to the piezo. The piezo can either control the height of the substrate relative to an immobilized cantilever or control the height of the cantilever relative to an immobilized substrate. Here we describe the procedure using nomenclature for the former method (as depicted in Fig. 33.1). There are two modes of motion for each pulling cycle (Fig. 33.4). In the up mode, initially the

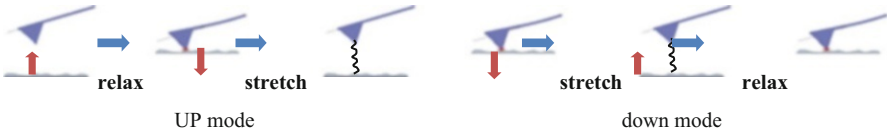

Fig. 33.4 Up mode versus down mode. *Red arrow* indicates the moving direction of the substrate; *blue arrow* indicates the process

tip rests above the surface; the pulling measurement starts with the substrate moving up first to bring into contact with the tip under a voltage ramp generated by the computer and then descending to the original position. While in the down mode, at first the tip presses slightly onto the substrate; the substrate begins to move down to leave the tip; and after that, the substrate reverts to the origin. The stretching traces in both modes are obtained when the substrate departs from the tip; accordingly the relaxing traces are acquired in the other half of the cycle.

Sometimes after the first cycle of pulling experiment, the cantilever tip still holds the molecule, which can be judged by discrepancy of the stretching trace tail from the horizontal line, since loss of the molecule would generate a horizontal baseline at the end of the stretching trace. Then refolding experiments can be realized by decreasing the pulling size to the desired length to stretch and relax the molecule for another several cycles.

Force–extension curves obtained from the AFM pulling experiments are selected first with several criteria and later analyzed with freely jointed chain (FJC) [73] or worm-like chain (WLC) [174] model for polymer elasticity. The FJC model considers the polymer chain segments (Kuhn segments) to be statistically independent. Assume that the elastic response of the polymer to the applied external force is purely entropic, then the extension $< x >$ (instant end-to-end distance of the polymer projected on the direction of the force) as a function of the applied force is

$$< x > = L_c \left(\coth \frac{F l_k}{k_B T} - \frac{k_B T}{F l_k} \right)$$

where L_c is the contour length of the molecule, l_k is Kuhn segment length of the polymer, T is the temperature, and k_B is the Boltzmann's constant. In reality, molecules are often overstretched so that enthalpic contributions to the extension originated from bending of covalent bond angles and elongation of covalent bonds have to be taken into account. The revised version of the FJC model is

$$< x > = L_c \left(\coth \frac{F l_k}{k_B T} - \frac{k_B T}{F l_k} \right) \left(1 + \frac{F}{k_{\text{segment}} L_c / N} \right)$$

where $k_{segment}$ is the so-called segment elasticity that includes all the enthalpic effects and N is the number of segments contained in the polymer chain.

The WLC model treats the polymer as an irregularly curved filament. In this model, the force versus extension $< x >$ relation is given by

$$F(< x >) = \frac{k_B T}{l_p} \left[\frac{1}{4} \left(1 - \frac{< x >}{L_c} \right)^2 + \frac{< x >}{L_c} - \frac{1}{4} \right]$$

where L_c is the contour length of the molecule and l_p is the persistent length of the polymer which equals one-half of l_k. In AFM studies, proteins are usually described using the WLC model, while DNA and sugar are depicted by revised FJC model.

The selection criteria for the force extension curve use a combination of heuristics. Often a reference fingerprint pattern of the unfolding for a protein is used. The fingerprint is obtained from a recording that has a number of force–extension recordings with enough unfolding events of the flanking protein handles and the correct initial contour length before the first unfolding. The theoretical value for initial contour length which precedes the first unfolding peak of the reference protein can be calculated out by the estimated length of the proteins when in their native form.

Protein Mechanics

Protein Unfolding

The sequence of amino acids in a protein encodes the unique three-dimensional structure which is attained through folding. Properly folded proteins are important for their function. The determination of the folding pattern of proteins from the amino acid sequence to the 3D structure is an important problem in biology. Proteins are characterized by their 3D structure, their function, and also by their dynamic processes such as unfolding and folding rates and progression to the native state. The folding and unfolding processes are stochastic although not all conformational transitions are equally possible as the energy landscape (the space of all conformations and associated free energies) is not flat. Each protein state has an energetic contribution from configurational entropy and enthalpy from forming hydrogen bonding or electrostatic networks. The states of the protein are also subject to environmental factors such as temperature and concentration of denaturants and mechanical forces, which all contribute to the energy landscape. Since it is currently experimentally unfeasible to monitor all possible order parameters, the multidimensional landscape of protein folding is often studied by looking at a single-order parameter (e.g., N–C extension, GdmCl concentration, percent of native contacts) which then describes a small part of the entire energy landscape. When proteins are perturbed using force, such as using AFM-SMFS, the order parameter is along the extension of protein, between the tethered ends (usually N–C extension). The relevant parameters that characterize protein unfolding by AFM-SMFS are the unfolding force, the contour length increment, the unfolding rate, the refolding rate, and the distance to the transition state. These properties for a wide variety of proteins are tabulated in Table 33.1 and each of these properties is discussed below, in detail.

A protein, upon mechanical unfolding (Fig. 33.5) by AFM or other SMFS tool, adopts an unstructured chain of amino acids that behave in a worm-like chain manner in which their bonds tend to line up with the vector of the pulling direction

Table 33.1 Compiled parameters for the unfolding of various proteins. The Protein Data Bank (PDB) code indicates the representative structure used to determine native state lengths and native contacts and fold type. The mean unfolding force, Fu, is determined from the comparable loading rates. Proteins with information about intrinsic unfolding rates, k_u^0; intrinsic folding rates (as determined by double-pulse protocol), k_f^0; and the distance to transition state, x_b, are included for respective proteins

Protein	References	PDB	F_u^a [pN]	ΔL_c [nm]	# aa	Fold type	k_u^0 [s^{-1}]	x_b [nm]	k_f^0 [s^{-1}]
Ankyrin repeat	[178–180]	2QYJ [181]	25–50	10.5–12.4	33	α			
Armadillo repeat	[182, 183]	2Z6H [184]	20–80	6.7, 15, 29.2	44	α			
Barnase	[185]	1A2P [186]	70	38	110	α/β			
Calmodulin	[187]	1CLL [188]	14	25,18.7	148	α	0.02	2	2×10^5
Cold-shock protein	[189]	1G6P [190]	78	23.5	64	β	1.5×10^{-2}	0.49	
Dihydrofolate reductase	[191]	1DLS [192]	82	67.4	186	α			
E2lip3 N–41	[176]	1QJO [193]	175	10	41	β	7.6×10^{-3}	0.29	
E2lip3 N–C	[176]	1QJO [193]	0	N/A	75	β			
Enhanced yellow fluorescent protein (EYFP) wild type	[194]	1YFP [195]	69	16,54	238	α/β			
EYFP circular permutant 145	[194]	N/A	68,103	13,57	238	α/β			
EYFP circular permutant 174	[194]	N/A	57,112	7,56	238	α/β			
Fibrinogen	[196]	N/A	90	23	112	α/β			
Protein G, B1 domain (GB1)	[197, 198]	2QMT [199]	178	17.7	56	α/β	3.9×10^{-2}	0.17	720
GB1 4,51- > His	[200]		120	17.7	56	α/β	1.2×10^{-1}	0.2	
GB1 6,53- > His	[200]		119	17.7	56	α/β	1.4×10^{-1}	0.2	
GB1 8,55- > His	[200]		160	17.7	56	α/β	2.9×10^{-2}	0.2	
Green fluorescent protein (3–212)	[201, 202]	1B9C [203]	105	77	227	α/β	7×10^{-2}	0.28	
HaloTag7	[171]	1BN6 [204]	106	66	187	α/β			

(*continued*)

Table 33.1 (continued)

Protein	References	PDB	F_u^a [pN]	ΔL_c [nm]	# aa	Fold type	k_u^0 [s^{-1}]	x_b [nm]	k_f^0 [s^{-1}]
Huntington elongation factor 3 protein phosphatase 2A and the yeast Kinase TOR1 (HEAT) repeat	[182]	1B89 [205]	20–75	5.8–16.1	29	α			
Ig rod domains of filamin from Dictyostelium discoideum (ddFLN4)	[206, 207]	N/A	62.9, 52.5	14.4, 16.6	98	β	0.28, 0.33	0.4, 0.52	55, 179
Kettin actin-binding region	[208]		193	30.1			9×10^{-3}	0.17	
Leucine rich (LR) repeat	[182]	2Q4G [209]	20–50		28	α/β			
Leucine zipper	[210]		10–15		43–95	α			
Maltose-binding protein	[211]	1ANF [212]	22,51, 25,20	22.6, 15.9, 42, 47.9	370	α/β	1.4×10^{-3}, 5.9×10^{-2}, 1000,10	2.3, 0.66,0.2, 0.38	
Myomesin	[213]	1R15 [214]	75	30	109	α/β			
Myosin coiled coil	[215, 216]		22–30 (plateau)	150–315		α			
Nebulin	[217]		220–1000	75–200	~6669	α			
NuG2 (protein G variant)	[218]	1MI0 [219]	105	15	56	α/β	3.1×10^{-2}	0.25	
Polycystin-1 (human) wild type	[220]	1B4R [221]	176		86	β	9.8×10^{-4}	0.25	
Polycystin-1 (human) mutant R57L	[220]		143		86	β	2.6×10^{-2}	0.24	
Polycystin-1 (human) mutant V59H	[220]		127		86	β	6.9×10^{-2}	0.22	
Polycystin-1 (human) mutant G43S	[220]		54		86	β	2.3×10^{-1}	0.31	

Projectin	[208]		90, 170	30.1			7×10^{-2}/0.3 $\times 10^{-3}$	0.1/0.2	15
Polycystin-1 (human) mutant T36C	[220]		79		86	β	0.7×10^{-1}	0.32	
Protein L	[222]	1HZ6 [223]	136	18.6	60	α	5×10^{-2}	0.22	
Scaffoldin c1C	[224]	1G1K [225]	430	48.5	144	β	1.1×10^{-4}	0.14	
Scaffoldin c2A	[224]	1ANU [226]	285	48.6	144	β	2.1×10^{-2}	0.15	
Scaffoldin c7A	[224]	1AOH [227]	562	49.3	144	β	6×10^{-6}	0.13	
Streptococcus pyogenes (Spy) 0128 E117A	[228]	3B2M [229]	172	52	142	β			
Streptococcus pyogenes (Spy) 0128 E258A	[228]	3B2M [229]	250	50	142	β			
Staphylococcal nuclease	[230]	2SNS [231]	26.3	47	149	α/β			
Small ubiquitin-related modifier 1	[232]	1A5R [233]	129	24.1	97	α/β	1.15×10^{-3}	0.51	
Small ubiquitin-related modifier 2	[232]	1WM3 [234]	122	24.1	93	α/β	5×10^{-3}	0.33	
Spectrin	[33, 65, 235, 236]	1S35 [237]	30	31.7	106	α	3.3×10^{-5}	1.7	
Synaptotagmin C2A	[238]	2R83 (140–265) [239]	51	39.6	126	β			
Synaptotagmin C2B	[238]	2R83 [239]	106	43	150	α/β			
T4 lysozyme	[240]	1 L63 [241]	64	55	103	α	5.5×10^{-2}	0.75	
Tenascin fibronectin domains all	[242]		138	24.7	88–92	β	4.6×10^{-4}	0.3	42, 0.5
Tenascin fibronectin type III domains	[243]	1TEN [244]	128	32.4	92	β			

(*continued*)

Table 33.1 (continued)

Protein	References	PDB	F_u[a] [pN]	ΔL_c [nm]	# aa	Fold type	k_u^0 [s^{-1}]	x_b [nm]	k_f^0 [s^{-1}]
Titin Ig27	[245]	1WAA [246]	200	28.5	89	β	3.3×10^{-4}	0.25	1.2
Titin kinase	[247]	1TKI [248]	40–120	9.1, 28.6, 7.3, 10.1, 7.5, 16.4, 58.3	344	α/β			
Titin-like protein TTN-1 Ig domain	[249]		85	30		β	5×10^{-2}	0.35	
Titin-like protein TTN-1 Ig/Fn domain	[249]		111	31		β	1.4×10^{-2}	0.35	
Titin-like protein TTN-1 kinase	[249]	1KOA [250]	83, 52	67, 97		α/β	4×10^{-2}	0.6	
Top7	[251]	1QYS [252]	150	29	92	α/β	6×10^{-2}	0.21	
Ubiquitin	[232, 253]	1UBQ [254]	188–203	24	76	α/β	8×10^{-3}	0.19	
Ubiquitin (48-C)	[253]		85	7.8	28	α/β			

[a]Note that these unfolding force values should be considered with care as they represent only the mean of many experiments. Force measurements between experiments may differ by up to 20 % due to uncertainty in the measurement of the spring constant of the cantilever [101]

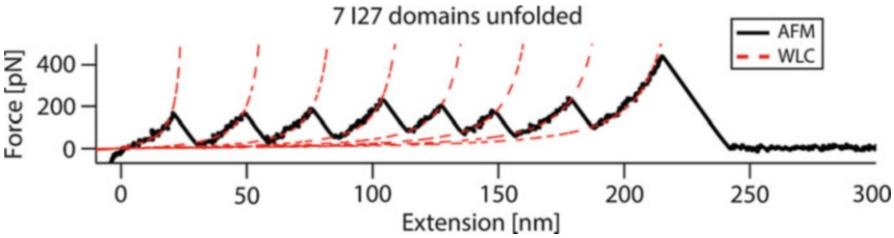

Fig. 33.5 Typical force–extension plot of the unfolding of a polyprotein consisting of seven I27 domains from the titin protein (also called I91 domains). Each peak corresponds to an unfolding event of a single domain. The unfolding force for each domain is ~200 pN. The dashed red line indicates a family of worm-like chain fits with a contour length spacing of 28.5 nm between unfolding events

with greater probability at higher force. Polyproteins will have several unfolding events as each protein domain contributes an unfolding event. The contour length distance between two unfolding events – as measured by the worm-like chain model – and the 3D crystal structure can be used to determine total extension of an amino acid at high force. For instance, the unfolding of a single I27 protein domain produces a contour length increment of 28.5 nm before the next unfolding event (Fig. 33.5). Before the rupturing of the single domain, it is assumed that the polyproteins have completely aligned with the pulling vector in their native state so that the extended chain distance is comprised of the increase in contour length (28.5 nm) plus the distance between the N-terminus and C-terminus of the protein in the native state, as measured by a NMR or X-ray crystal structure model (4 nm for IgI27). Thus, the total length 28.5 nm + 4 nm = 32.5 nm divided by the number of amino acids, 89, gives the distance of a fully extended single amino acid unit of IgI27, which is 3.65 Å. The mean length of a fully extended amino acid unit determined from the corresponding proteins in Table 33.1 with their corresponding PDB structures is 3.64 ± 0.04 Å (mean ± SE, n = 27). The consistency between these measurements then allows for the contour length increment, $\Delta L_{c,}$ to be an important indicator of the number of amino acids unfolding within each unfolding event, if the protein structure is known, by inverting the previous calculation.

The unfolding force, F_u, for proteins ranges from as low as 5 pN up to 500 pN. The nonzero unfolding force is the result of proteins resisting unfolding due to an energy barrier between the unfolded and folded state along the particular pathway. The likelihood of unfolding increases exponentially with applied force because of thermal activation of bond rupturing so that the unfolding force is logarithmically dependent on the loading rate (cantilever stiffness x pulling velocity) [175]. The model derived from this concept, called the Bell–Evans–Ritchie model, interprets the log-linear dependence of the loading rate with force as an image of an energy barrier at a fixed location along the pathway. The intrinsic unfolding rate, k_u^0, can then be determined by relating natural logarithm of the loading rate, *r*, to the most likely unfolding force, F_u, with the formula

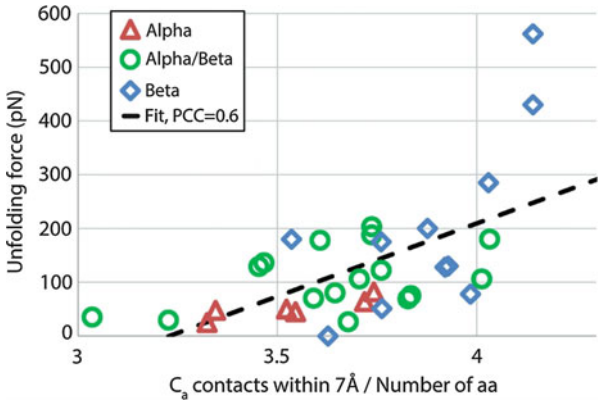

Fig. 33.6 There is a correlation between the density of contacts and the unfolding force as determined by the Pearson correlation coefficient (PCC). Alpha-helical proteins exhibit the lowest unfolding forces and beta-folds exhibit higher unfolding forces but are geometry dependent

$$F_u(r) = \frac{k_b T}{x_b} ln\left(\frac{r x_b}{k_u^0 k_b T}\right).$$

This model incorporates the parameter x_b, which corresponds to the distance to the fixed location along the pathway from the unfolding state and the top of the barrier (the transition state). The experiments to determine these parameters are often referred to as "dynamic force spectroscopy" which simply involves performing pulling experiments at many loading rates (differing speeds and varying strengths of cantilever spring constants) to get enough data to reliably fit the parameters in the Bell–Evans–Ritchie model.

The intrinsic folding rate of proteins, k_f^0, can be determined using a polyprotein and a "double-pulse" protocol. In this experiment, a polyprotein is unfolded during the first pulse and the number of unfolded modules determined. Then, after waiting a time *t*, a second pulse is applied and the number of modules unfolded is counted. The modules unfolded in the second pulse were able to refold during the time delay *t*. Thus, the proportion of the refolded protein modules out of the total unfolded modules in the first pulse can be plotted against the time delay *t* and fit to an exponential function to determine the intrinsic folding rate for each module, k_f^0. The 3D structure and geometry of the pulling vectors also affects the unfolding force of proteins [176, 177]. However, most proteins unfolded from the N-terminus to the C-terminus have an unfolding force that correlates with contact density and their specific fold type (Fig. 33.6).

It would be useful to determine the unfolding parameters of proteins from pulling experiments through computer simulations and purely theoretic means since many proteins already have a 3D structure available and experimental setups can be time intensive and costly. The atomistic detail of molecular dynamic simulations also provides insightful explanations for unfolding and folding phenomena. The analogous computer simulation to the experimental force spectroscopy experiment is steered molecular dynamics [255]. Steered molecular

Table 33.2 Tabulated peak unfolding forces from steered molecular dynamic simulations with explicit water and comparable force fields (OPLS-AA or CHARM22 or AMBER99). Unfolding forces were compared at a pulling speed of 100 A/ns. Unfolding forces from simulations performed at other were extrapolated to 100 A/ns using unfolding force peaks from at least three different speeds fitted using log-linear regression (in accordance with Bell–Evans–Ritchie model where unfolding force depends on the logarithm of speed)

Protein	References	Simulated peak unfolding force [pN]
Barnase	[256]	1048[a]
Fibronectin III domain	[257, 258]	1231[a]
NI6C	[259]	245[b]
Scaffoldin c1C	[224]	2253[a]
Scaffoldin c2A	[224]	1420[a]
Scaffoldin c7A	[224]	2236[a]
Spectrin	[260]	457[a]
Titin I27	[224, 251, 261]	1460
Top7	[251]	1050
Ubiquitin (48-C)	[253]	1400
Ubiquitin (N–C)	[253]	2000

[a]Extrapolated to 100 A/ns using several speeds
[b]5A/ns

dynamics consists of a solvated protein model (determined from X-ray crystallography or NMR) that is fixed at one end and pulled at constant velocity or constant force on the other. These simulations do not reach the quasi-equilibrium conditions of the actual experiments because of limitations in computing time. Thus, the unfolding of proteins in steered molecular dynamics simulations are performed at speeds that are orders of magnitude faster. Table 33.2 lists the simulated peak unfolding force determined from the steered molecular dynamic simulations. Even though computer simulations are done at much higher speeds, there is a good correlation between the experimental results of the unfolding force and the theoretical unfolding force determined through simulation, as shown in Fig. 33.7.

Protein–Ligand Complex Unfolding

Proteins bind to cofactors and other proteins which can have an effect on their mechanical stability (as perturbed from the N to C extension) as tabulated in Table 33.3. In all cases the unfolding force is increased upon binding with the exception of titin kinase in which a new separate unfolding event occurred in the presence of ligand. Dr. Hongbin Li and colleagues exploited the difference between apo- and bound force spectra of proteins and measured the dissociation constant of proteins with their ligands by counting the proportion of bound proteins based on their unfolding force [30, 72, 73]. Surprisingly, the dissociation constants for

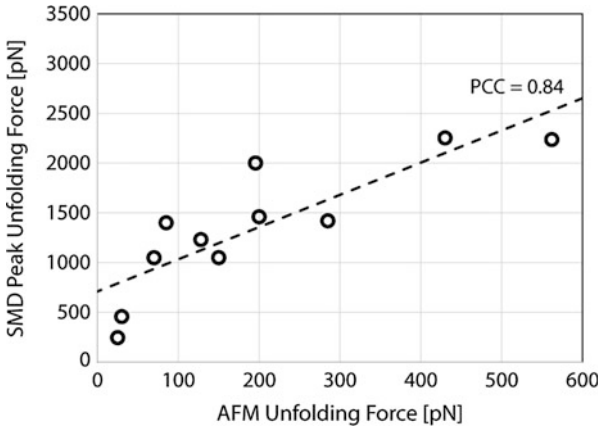

Fig. 33.7 Correlation between unfolding forces as performed by steered molecular dynamics (y-axis; from Table 33.2) and experimentally determined by atomic force microscopy (x-axis from Table 33.1). The correlation between the datasets is 0.84 determined by the Pearson correlation coefficient

Table 33.3 Protein unfolding characteristics when bound to their respective ligands. The fold increase indicates the increase in the mean unfolding force from the unfolding force tabulated in Table 33.1. The dissociation constant, Kd, was measured from SMFS experiments for some protein–ligand combinations and compared to the bulk measure dissociation constant (*italics*)

Protein	References	Ligand	F_u increase [fold increase]	K_d [M] (*bulk K_d [M]*)
Calmodulin	[187]	10 μM Mas peptide	1.4×	
DHFR	[191]	19 μM–1.2 mM MTX	2.9×	
DHFR	[191]	180 μM DHF	3.1×	
DHFR	[191]	210 μM NADPH	3.4×	
GB1 4,51- > His	[200]	4 mM Ni^{2+}	1.7×	
GB1 6,53- > His	[200, 262]	4 mM Ni^{2+}	2.0×	9.8×10^{-5} (*2.6×10^{-4}*)
GB1 8,55- > His	[200]	4 mM Ni^{2+}	1.4×	
GB1	[263]	hFc antibody	1.5×	2.2×10^{-6} (*5×10^{-10}–5×10^{-7}*)
Maltose-binding protein (53–141)	[264]	Maltose	1.1×	
NuG2	[263]	hFc antibody	2.0×	1.3×10^{-5} (*5×10^{-10}–5×10^{-7}*)
Staphylococcal nuclease	[230]	Deoxythymidine 3',5'-bisphosphate	1.9×	
Titin kinase	[247]	ATP	N/A[a]	3.5×10^{-4} (*2.4×10^{-4}*)

[a]Instead of increasing unfolding force, an additional peak appears

proteins and their antibodies are lower than when measured with traditional experimental methods, while the dissociation constants for metal ions or small molecules are comparable. The differences between the SMFS measured dissociation constant and the bulk measured constant may be due to the mechanical perturbations required in SMFS, but more research in this area is needed.

Protein–Ligand Unbinding

The model for measuring the energy barrier between the folded state and the unfolded state of proteins can also be applied to the energy barrier between the bound and unbound state of proteins with their ligand. In these experiments the protein is conjugated to the tip and the ligand is conjugated to a surface. Pulling experiments are then performed and all the unbinding forces are recorded and tabulated in a histogram. The control experiment where there is no ligand conjugated to the surface serves as a distribution of nonspecific binding forces. Performing measurements at varying loading rates can determine the unbinding rate using the Bell–Evans–Ritchie model discussed in Section IIIA which can be used to extrapolate a dissociation constant for a protein and its ligand. The unbinding forces for several protein–ligand complexes and their dissociation constants (when known) are shown in Table 33.4. The unbinding forces range from 30 pN to 250 pN. The association constants (inverse of the dissociation constant) are positively correlated with the binding force as shown in Fig. 33.8.

Protein-Based Nanomaterials

The properties of proteins lend themselves to be useful building blocks for nanomaterials. Individual proteins can be selected based on mechanical strength and elastic characteristics and then fused at the DNA level into polyproteins. These polyproteins can then be linked via thiol chemistry or protein chemistry into biomaterials. Hongbin Li and colleagues tested this idea by building a protein-based elastomeric hydrogel ring constructed from a network of polyprotein GB1 domains [283]. The properties of the material can then be easily tuned by changing the composition of the polyproteins. Such materials are useful for developing scaffolds for tissue engineering.

DNA

The behavior of DNA under force has been studied for over 30 years using a variety of techniques. Single-molecule methods have allowed for precise characterization of DNA under force which revealed mechanical transitions that occur during unwinding and melting of the DNA helix [32, 284–292]. The origin of these transitions is still under study. One of the first DNA molecules studied is the λ phage dsDNA molecule, composed of 48,502 bp. When force is exerted on both ends of the molecule, it stretches and the force increases following the worm-like chain model very closely at forces below 50 pN. The force–extension profile is salt dependent, and measurements in 10 mM Na+ typically indicate a persistence length of ~60 nm and an elastic modulus of ~800 pN as shown in Table 33.5.

The λ phage DNA, along with other types of double-stranded DNA and single-stranded DNA/RNA, has been shown to undergo overstretching transitions when

Table 33.4 Tabulated unbinding forces for protein–ligand rupture events from SMFS. SMFS can also be used to determine the experimental dissociation constant, K_d, from single molecules perturbed by force (in contrast to the dissociation constant measured from a bulk sample in italic)

Protein–ligand	References	Unbinding force [pN]	K_d [M] (*bulk* K_d [*M*])
Alpha-synuclein/alpha-synuclein (with spermidine)	[265]	60	
Amyloid β-40 peptide/amyloid β-40 peptide	[266]	100	
Amyloid β-42 peptide/amyloid β-42 peptide	[267]	41, 47 (with Cu^{2+})	
Antifluorescein Fv fragment/fluorescein	[268]	160	2.4×10^{-9} (1.1×10^{-9})
Antilysozyme Fv fragment/lysozyme	[269]	55	(3.7×10^{-9})
Anti-Sendai antibody/Sendai bacteriorhodopsin	[270]	126	
Azurin/cytochrome c551	[271]	95	(1×10^{-5})
Biotin–avidin	[272]	80	(1×10^{-15})
Cadherin/cadherin X-dimer	[273, 274]	35	(1×10^{-4})
Cadherin/cadherin strand-swapped dimer	[274]	55	
ExpG protein/DNA target sequence	[275]	75	
HSA (human serum albumin)/anti-HSA	[276]	244	
Ni^{2+}-NTA/histidine peptide	[277]	38	(1.4×10^{-8})
p53/azurin	[278]	75	6×10^{-6} (3.3×10^{-8})
P-selectin/ligand	[279]	115	5.5×10^{-8} (6×10^{-8})
RNase inhibitor/angiogenin	[280]	78,156	(5×10^{-7}, 7×10^{-16})
Streptavidin/biotin	[172]	253	(1×10^{-14})
Strep-Tactin/Strep-tag II	[280, 281]	40–48,74	(1×10^{-6})
Titin Z1 and Z2 dimerization	[282]	700	

stretched beyond 15 pN up to 1800 pN. The origin of these transitions is still a subject of study. The transition forces and gain in extension (as determined by normalized extensions) are shown in Table 33.6.

Sugars

Entropic Elasticity and Force-Induced Conformational Transitions of Polysaccharides

AFM proved very valuable for characterizing the mechanical properties of many polysaccharides and enabled observations of unique force-driven transitions in the sugar rings [73, 83, 98, 308–310]. For AFM measurements, a polysaccharide sample

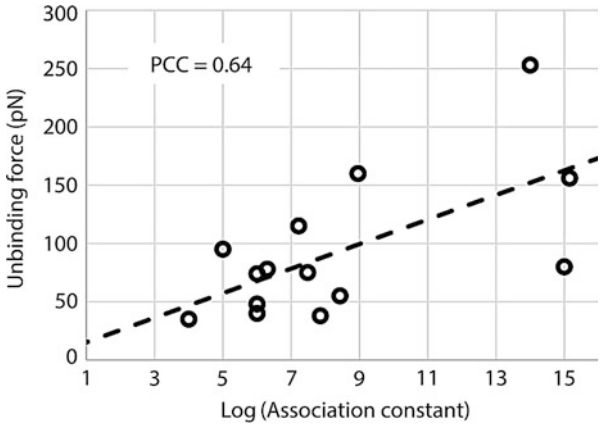

Fig. 33.8 The unbinding force at similar load rates for proteins and their ligands correlates with the bulk measured association constant (inverse of dissociation constant)

Table 33.5 Basic properties of λ phage DNA as studied by a variety of nanomolecular techniques

Method	References	Ionic strength [mM Na+]	Persistence length[a] [nm]	Elastic modulus [pN]
SMFS-laser tweezers	[293–295]	9–10	53–67	452–1008
Magnetic tweezers	[296]	10	53	869
AFM compression	[297]	N/A	N/A	700
SMFS-AFM	[298]	N/A	N/A	558

[a]These values should be treated with caution as the exact value of the persistence length of dsDNA is a matter of controversy, and the newest study [299] suggests that this value may be significantly lower than the values shown in the table

is dissolved in water or another appropriate solvent at a wide range of concentrations ranging from 0.001 % to 20 % (w/w). A small drop of the solution (e.g., 50–100 μl) is placed on a clean substrate (glass, gold) and the molecules are allowed to adsorb to the substrate for several hours. The nonattached or weakly attached molecules are then removed from the surface by vigorous washing of the substrate. The molecules that strongly adsorbed to the substrate can then be lifted from it by the AFM tip and stretched in solution so their extension and tension can be accurately measured [90].

While some polysaccharides display the entropic elasticity that is typical of many structurally simple polymers at all forces (e.g., cellulose [308, 311]), some polysaccharides follow this behavior only at low forces, and at higher forces they show marked deviations from the entropic elasticity (e.g., amylose, dextran, pectin [83, 312]). These deviations are caused by force-induced conformational transitions within the sugar rings (e.g., chair–boat transitions in α-D-glucopyranose [98]), within the bonds connecting neighboring rings (e.g., bond flips in pustulan [313, 314]) or by force-induced separation of polysaccharide chains in multichain molecular structures (e.g., xanthan [315, 316]). Generally, when sugar monomers are connected by equatorial glycosidic linkages that lay in the plane of the sugar ring

Table 33.6 Properties of nucleic acid polymers when perturbed by forces up to 1.8nN. Nomenclature: poly(dA) stands for a polymer of polydeoxyadenylic acid, or a single-stranded DNA molecule composed only of adenines whereas poly(A) stands for a polymer of polyadenylic acid, which consists of a single-stranded RNA molecule composed of adenines. Similarly, poly(dGdC)poly(dCdG) stands for a double-stranded DNA composed of CG repeats. Overstretching percent refers to the percent fraction of the plateau relative to the initial length

Nucleic acid	References	Canonical form[a]	1st plateau [pN]	Overstretching [%]	2nd plateau [pN]	Overstretching [%]
Poly(dA)	[300, 301]	B-helix	23	80	113	16
Poly(A)	[302, 303]	A-helix	24	80	-	-
Poly(C)	[303]	A-helix	25	~50	-	-
Poly(dT)	[300]	Unstructured	-	-	-	-
Poly(U)	[303]	Unstructured				
dsDNA (e.g., lambda phage DNA)	[96, 284, 286, 288, 289, 304–306]	B-helix	65–105	70	150–450	10–20
Poly(dGdC) poly(dCdG)	[305, 306]	B-helix	65–95	70	300–450	20
Poly(dG) poly(dC)	[306]	A-helix	70	70	-	-
Poly(dA) poly(dT)	[306]	B'-helix	70	70		
Poly(dAdT) poly(dTdA)	[304, 305]	D-helix	35	-	-	-

[a]See reference [307] for specific characteristics of DNA helixes

(as in cellulose), the elasticity of these polysaccharides is primarily entropic in nature and force spectra are quite simple. When monomers are connected by axial bonds (that are perpendicular to the plane of the sugar ring), the elasticity of those polysaccharides frequently displays interesting features (deviations) from the entropic elasticity that manifest themselves as pronounced force plateaus. Those plateaus were interpreted as indicative of force-induced transitions of the sugar ring from a low-energy conformation to a high-energy conformation that provides an increased separation of the consecutive glycosidic oxygen atoms and thus increases the contour length of the chain. Force bond rotations (flips) that occur over an energy barrier (such as in 1,6 linked polysaccharides) typically produce linear relationships between force and extension. Unwinding of helical structures (such as in xanthan) typically produces a long plateau in the force extension data and is typically associated with pronounced hysteresis between the stretching and relaxing part of the force–extension spectrum that reports strand separation in multiple helices. Table 33.7 compiles most of the known elasticity profiles (force spectrums) of various natural polysaccharides measured by AFM, in solution, on isolated molecules. The elasticity profiles of a number of polysaccharides measured directly on cell surfaces, from which they protrude, may be found through the references in a recent review [83].

Table 33.7 Table of sugars and their corresponding chemical structures and force spectra as determined by atomic force microscopy

Polysaccharide	Chemical structure	Force spectrum	References
Amylose	α-1,4 D-glucopyranose 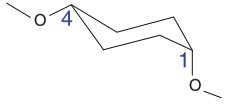	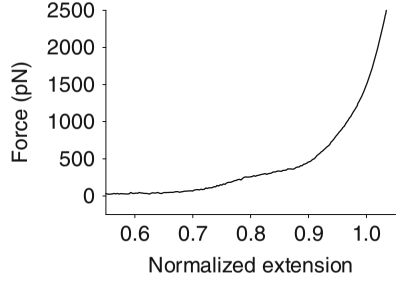	[98, 309, 311, 317–322]
Dextran	α−1,6 D-glucopyranose 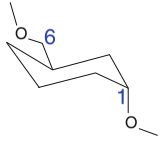	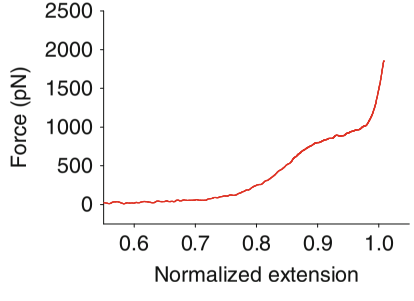	[73, 98, 317, 323]

(*continued*)

Table 33.7 (continued)

Polysaccharide	Chemical structure	Force spectrum	References
Pullulan	[2(α-1,4) + α1,6]$_n$ D-glucopyranose 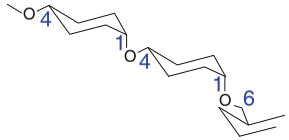	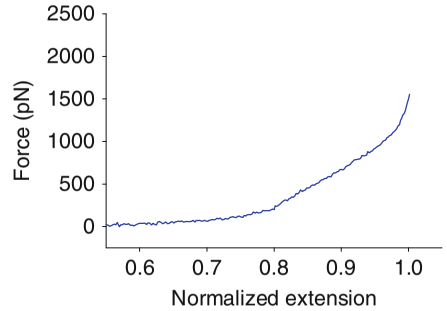	[98, 317]
Pectin	α-1,4 D-galactopyranuronic acid 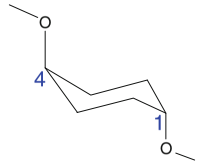	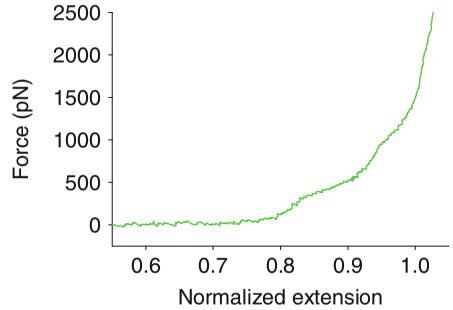	[308]

Cellulose	β-1,4 D-glucopyranose		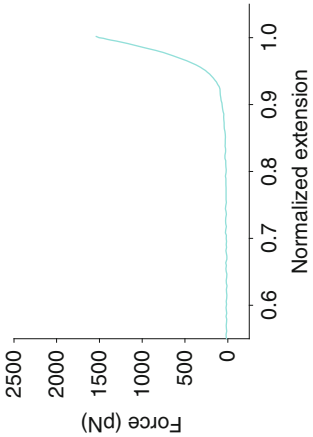	[308, 311, 316]
Beta-galactan	β-1,4 D-galactopyranose	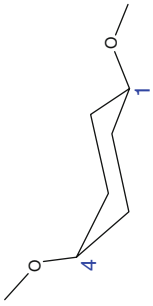	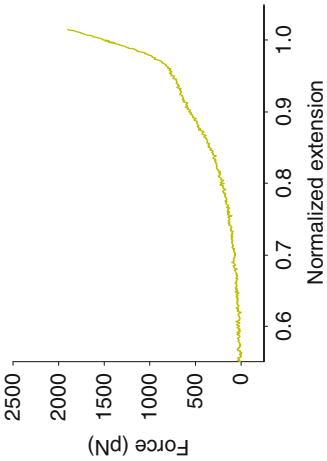	[324]

(*continued*)

Table 33.7 (continued)

Polysaccharide	Chemical structure	Force spectrum	References
Pustulan	β-1,6 D-glucopyranose 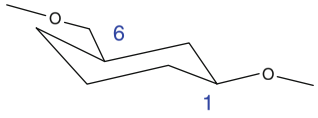	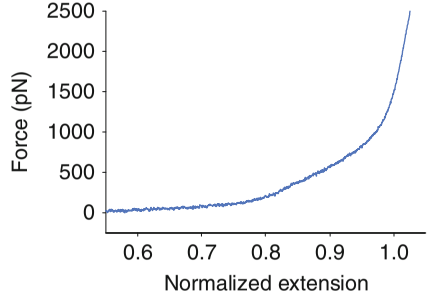	[313]
Carrageenan λ	[(α-1,3) + (β1,4)]n D-galactopyranose 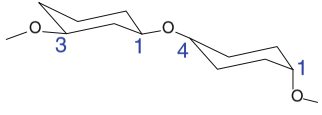	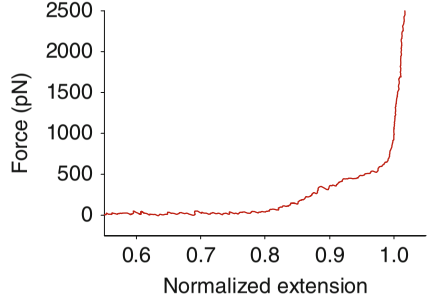	[317, 325]

Carrageenan ι (iota)	[(α−1,3) + (β1,4)]n D-galactopyranose 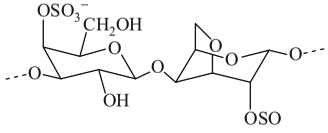	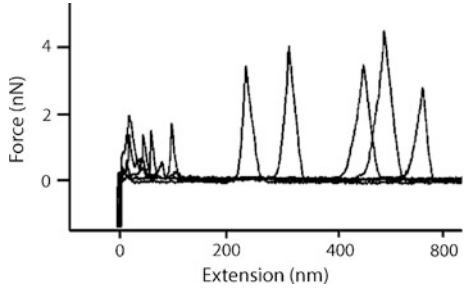	[325]
Alginate Poly(GM)	(Poly GM; 40 %G + 60 %M): α-1,4 L-glucopyranuronic acid (G) + β-1,4 D-mannuropyranuronic acid (M) 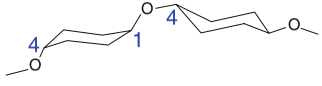	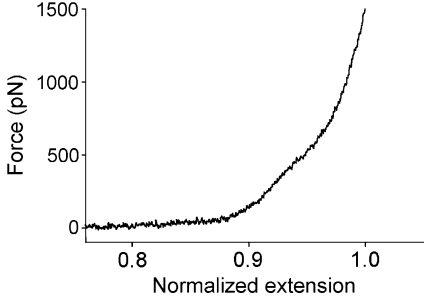	[312]

(*continued*)

Table 33.7 (continued)

Polysaccharide	Chemical structure	Force spectrum	References
Alginate Poly(M)	β-1,4 D-mannuropyranuronic acid 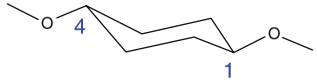	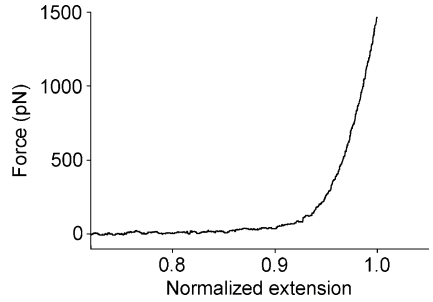	[312]
Heparin	Uronic acid, and α glucose-amine or α galactosamine sugar linked by α (1,4) or β (1,3) linkages 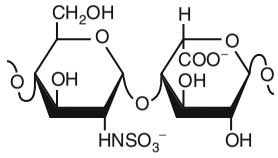	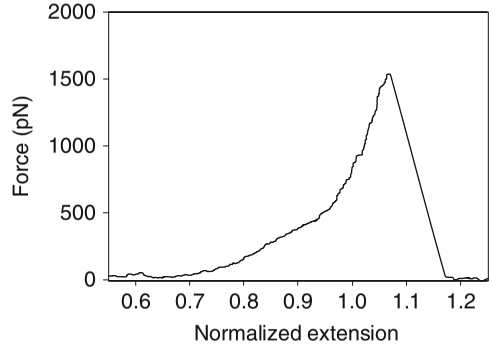	[311, 326]

Curdlan	β-(1,3)-linked D-glucose 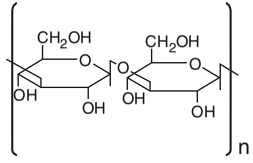	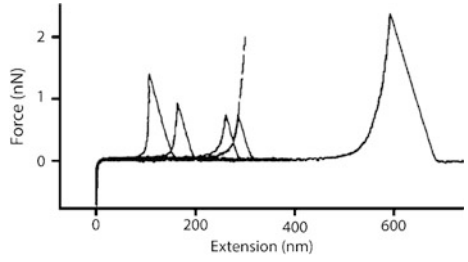	[327]
Xanthan	A linear cellulosic backbone of (1,4)-β-D-glucose substituted with a trisaccharide side chain O-β-D mannopyranosyl-(1,4)-O-β-D-glucopyranosyl-uronic acid-(1,2)-6-O-acetyl-α-D-mannopyranosyl at the C-3 of alternate glucose residues of the main chain	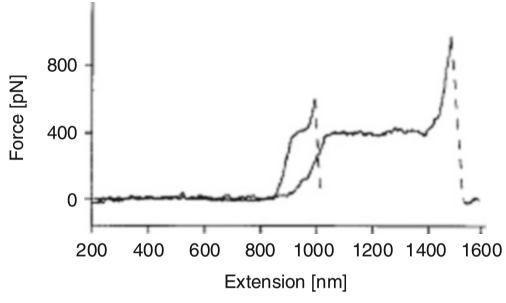	[316]

Outlook and Conclusion

The development of single-molecule manipulation techniques over the last 20 years enabled direct measurements of the mechanical properties of individual biomacromolecules. The number of biopolymers tested is steadily increasing and many fundamental observations and measurements were already repeated on the same systems by independent groups and verified. The data about types of elasticity and force-induced structural transitions obtained this way is invaluable for deciphering molecular mechanisms supporting life processes and for using these biopolymers in nanobiotechnology. Standardization of measurement conditions, automation of measurements [328] and analysis, and improvements of the accuracy of force sensors calibration [329] will continue to increase the quantity and reliability of single-molecule characterization measurements.

Acknowledgments The authors would like to acknowledge funding support from NSF MCB-1052208.

References

1. Seeman NC (2003) DNA in a material world. Nature 421(6921):427–431
2. Seeman NC (2005) From genes to machines: DNA nanomechanical devices. Trends Biochem Sci 30(3):119–125. doi:10.1016/j.tibs.2005.01.007
3. Seeman NC (2007) An overview of structural DNA nanotechnology. Mol Biotechnol 37(3):246–257. doi:10.1007/s12033-007-0059-4
4. Seeman NC (2010) Nanomaterials based on DNA. Annu Rev Biochem 79:65–87. doi:10.1146/annurev-biochem-060308-102244
5. Seeman NC, Belcher AM (2002) Emulating biology: building nanostructures from the bottom up. Proc Natl Acad Sci USA 99(Suppl 2):6451–6455. doi:10.1073/pnas.221458298
6. Ito Y, Fukusaki E (2004) DNA as a 'nanomaterial'. J Mol Catal B: Enzym 28(4–6):155–166. doi:10.1016/j.molcatb.2004.01.016
7. Zhang SG (2003) Fabrication of novel biomaterials through molecular self-assembly. Nat Biotechnol 21(10):1171–1178. doi:10.1038/nbt874
8. Gothelf KV, LaBean TH (2005) DNA-programmed assembly of nanostructures. Org Biomol Chem 3(22):4023–4037. doi:10.1039/b510551j
9. Davis JT, Spada GP (2007) Supramolecular architectures generated by self-assembly of guanosine derivatives. Chem Soc Rev 36(2):296–313. doi:10.1039/b600282j
10. Bath J, Turberfield AJ (2007) DNA nanomachines. Nat Nanotechnol 2(5):275–284. doi:10.1038/nnano.2007.104
11. Aldaye FA, Palmer AL, Sleiman HF (2008) Assembling materials with DNA as the guide. Science 321(5897):1795–1799. doi:10.1126/science.1154533
12. Zhang DY, Seelig G (2011) Dynamic DNA nanotechnology using strand-displacement reactions. Nat Chem 3(2):103–113. doi:10.1038/nchem.957
13. Pinheiro AV, Han D, Shih WM, Yan H (2011) Challenges and opportunities for structural DNA nanotechnology. Nat Nanotechnol 6(12):763–772. doi:10.1038/nnano.2011.187
14. Adleman LM (1994) Molecular computation of solutions to combinatorial problems. Science 266(5187):1021–1024. doi:10.1126/science.7973651
15. Adleman LM (1998) Computing with DNA. Sci Am 279(2):54–61

16. Braich RS, Chelyapov N, Johnson C, Rothemund PWK, Adleman L (2002) Solution of a 20-variable 3-SAT problem on a DNA computer. Science 296(5567):499–502. doi:10.1126/science.1069528
17. Liu QH, Wang LM, Frutos AG, Condon AE, Corn RM, Smith LM (2000) DNA computing on surfaces. Nature 403(6766):175–179
18. Benenson Y, Adar R, Paz-Elizur T, Livneh Z, Shapiro E (2003) DNA molecule provides a computing machine with both data and fuel. Proc Natl Acad Sci USA 100(5):2191–2196. doi:10.1073/pnas.0535624100
19. Smith BL, Schaffer TE, Viani M, Thompson JB, Frederick NA, Kindt J, Belcher A, Stucky GD, Morse DE, Hansma PK (1999) Molecular mechanistic origin of the toughness of natural adhesives, fibres and composites. Nature 399(6738):761–763
20. Thompson JB, Kindt JH, Drake B, Hansma HG, Morse DE, Hansma PK (2001) Bone indentation recovery time correlates with bond reforming time. Nature 414(6865):773–776
21. Gutsmann T, Fantner GE, Kindt JH, Venturoni M, Danielsen S, Hansma PK (2004) Force spectroscopy of collagen fibers to investigate their mechanical properties and structural organization. Biophys J 86(5):3186–3193. doi:S0006-3495(04)74366-0 [pii], doi:10.1016/S0006-3495(04)74366-0
22. Oroudjev E, Soares J, Arcdiacono S, Thompson JB, Fossey SA, Hansma HG (2002) Segmented nanofibers of spider dragline silk: atomic force microscopy and single-molecule force spectroscopy. Proc Natl Acad Sci USA 99(14):9606. doi:10.1073/pnas.132282899 (Proc Natl Acad Sci USA 99:6460)
23. Oroudjev E, Soares J, Arcdiacono S, Thompson JB, Fossey SA, Hansma HG (2002) Segmented nanofibers of spider dragline silk: atomic force microscopy and single-molecule force spectroscopy. Proc Natl Acad Sci USA 99:6460–6465. doi:10.1073/pnas.082526499
24. Oroudjev EM, Hansma HG (2002) AFM and force spectroscopy of recombinant spider dragline silk protein nanofibers. Biophys J 82(1):41A–42A
25. Cao Y, Li H (2007) Polyprotein of GB1 is an ideal artificial elastomeric protein. Nat Mater 6(2):109–114, http://www.nature.com/nmat/journal/v6/n2/suppinfo/nmat1825_S1.html
26. Cao Y, Li H (2008) Engineered elastomeric proteins with dual elasticity can be controlled by a molecular regulator. Nat Nanotechnol 3(8):512–516
27. Li HB, Cao Y (2010) Protein Mechanics: from single molecules to functional biomaterials. Acc Chem Res 43(10):1331–1341. doi:10.1021/ar100057a
28. Lv S, Dudek DM, Cao Y, Balamurali MM, Gosline J, Li H (2010) Designed biomaterials to mimic the mechanical properties of muscles. Nature 465(7294):69–73, http://www.nature.com/nmat/journal/v6/n2/suppinfo/nmat1825_S1.html
29. Kim M, Wang C-C, Benedetti F, Rabbi M, Bennett V, Marszalek PE (2011) Nanomechanics of Streptavidin hubs for molecular materials. Adv Mater 23(47):5684–5688. doi:10.1002/adma.201103316
30. Robyt JF (1998) Essentials of carbohydrate chemistry. Springer-Verlag, New York, p 163
31. Rao VSR, Qasba PK, Balaji PV, Chandrasekaran R (1998) Conformation of carbohydrates. Harwood Academic Publishers, The Netherlands
32. Bustamante C, Bryant Z, Smith SB (2003) Ten years of tension: single-molecule DNA mechanics. Nature 421(6921):423–427
33. Bao G, Suresh S (2003) Cell and molecular mechanics of biological materials. Nat Mater 2(11):715–725. doi:10.1038/nmat1001
34. Bennett V, Baines AJ (2001) Spectrin and Ankyrin-based pathways: Metazoan inventions for integrating cells Into tissues. Physiol Rev 81(3):1353–1392
35. Benoit M, Gaub HE (2002) Measuring cell adhesion forces with the atomic force microscope at the molecular level. Cells Tissues Organs 172(3):174–189
36. Deguchi S, Ohashi T, Sato M (2006) Tensile properties of single stress fibers isolated from cultured vascular smooth muscle cells. J Biomech 39(14):2603–2610

37. del Rio A, Perez-Jimenez R, Liu RC, Roca-Cusachs P, Fernandez JM, Sheetz MP (2009) Stretching single talin rod molecules activates vinculin binding. Science 323(5914):638–641. doi:10.1126/science.1162912
38. Emerson RJ IV, Camesano TA (2004) Nanoscale investigation of pathogenic microbial adhesion to a biomaterial. Appl Environ Microbiol 70(10):6012–6022. doi:10.1128/aem.70.10.6012-6022.2004
39. Evans E (2001) Probing the relation between force – Lifetime – and chemistry in single molecular bonds. Annu Rev Biophys Biomol Struct 30:105–128. doi:10.1146/annurev.biophys.30.1.105
40. Evans E, Ritchie K (1997) Dynamic strength of molecular adhesion bonds. Biophys J 72(4):1541–1555
41. Evans E, Ritchie K, Merkel R (1995) Sensitive force technique to probe molecular adhesion and structural linkages at biological interfaces. Biophys J 68(6):2580–2587
42. Evans EA, Calderwood DA (2007) Forces and bond dynamics in cell adhesion. Science 316(5828):1148–1153. doi:10.1126/science.1137592
43. Florin E, Moy V, Gaub H (1994) Adhesion forces between individual ligand-receptor pairs. Science 264(5157):415–417. doi:10.1126/science.8153628
44. Grashoff C, Hoffman BD, Brenner MD, Zhou R, Parsons M, Yang MT, McLean MA, Sligar SG, Chen CS, Ha T, Schwartz MA (2010) Measuring mechanical tension across vinculin reveals regulation of focal adhesion dynamics. Nature 466(7303):263–266. doi: http://www.nature.com/nature/journal/v466/n7303/abs/nature09198.html#supplementary-information
45. Hanley W, McCarty O, Jadhav S, Tseng Y, Wirtz D, Konstantopoulos K (2003) Single molecule characterization of P-selectin/ligand binding. J Biol Chem 278(12):10556–10561
46. Helenius J, Heisenberg CP, Gaub HE, Muller DJ (2008) Single-cell force spectroscopy. J Cell Sci 121(11):1785–1791. doi:10.1242/jcs.030999
47. Kienberger F, Ebner A, Gruber HJ, Hinterdorfer P (2006) Molecular recognition imaging and force spectroscopy of single biomolecules. Acc Chem Res 39(1):29–36. doi:10.1021/ar050084m
48. Krammer A, Craig D, Thomas WE, Schulten K, Vogel V (2002) A structural model for force regulated integrin binding to fibronectin's RGD-synergy site. Matrix Biol 21(2):139–147
49. Krammer A, Lu H, Isralewitz B, Schulten K, Vogel V (1999) Forced unfolding of the fibronectin type III module reveals a tensile molecular recognition switch. Proc Natl Acad Sci USA 96(4):1351–1356
50. Leckband D, Prakasam A (2006) Mechanism and dynamics of cadherin adhesion. Ann Rev Biomed Eng 8(1):259–287, 10.1146/annurev.bioeng.8.061505.095753
51. Leckband D, Sivasankar S (2012) Cadherin recognition and adhesion. Curr Opin Cell Biol 24(5):620–627. doi:10.1016/j.ceb.2012.05.014
52. Leckband D, Sivasankar S (2012) Biophysics of cadherin adhesion. In: Harris T (ed) Adherens junctions: from molecular mechanisms to tissue development and disease, vol 60, Subcellular biochemistry. Springer, Netherlands, pp 63–88. doi:10.1007/978-94-007-4186-7_4
53. Lee H, Scherer NF, Messersmith PB (2006) Single-molecule mechanics of mussel adhesion. PNAS 103(35):12999–13003. doi:10.1073/pnas.0605552103
54. Li F, Redick SD, Erickson HP, Moy VT (2003) Force measurements of the α5β1 integrin–fibronectin interaction. Biophys J 84(2):1252–1262. doi:10.1016/s0006-3495(03)74940-6
55. Litvinov RI, Shuman H, Bennett JS, Weisel JW (2002) Binding strength and activation state of single fibrinogen-integrin pairs on living cells. Proc Natl Acad Sci 99(11):7426–7431. doi:10.1073/pnas.112194999
56. Liu W, Montana V, Parpura V, Mohideen U (2009) Single molecule measurements of interaction free energies between the proteins within binary and ternary SNARE complexes. J Nanoneuroscience 1(2):120–129. doi:10.1166/jns.2009.1001

57. Liu Y, Pinzón-Arango PA, Gallardo-Moreno AM, Camesano TA (2010) Direct adhesion force measurements between E. coli and human uroepithelial cells in cranberry juice cocktail. Mol Nutr Food Res 54(12):1744–1752. doi:10.1002/mnfr.200900535
58. Liu Y, Strauss J, Camesano TA (2008) Adhesion forces between *Staphylococcus epidermidis* and surfaces bearing self-assembled monolayers in the presence of model proteins. Biomaterials 29(33):4374–4382. doi:10.1016/j.biomaterials.2008.07.044
59. Ludwig M, Moy VT, Rief M, Florin EL, Gaub HE (1994) Characterization of the adhesion force between avidin-functionalized Afm tips and biotinylated agarose beads. Microscop Microanal Microstruct 5(4–6):321–328
60. Marshall BT, Long M, Piper JW, Yago T, McEver RP, Zhu C (2003) Direct observation of catch bonds involving cell-adhesion molecules. Nature 423(6936):190–193
61. Ng SP, Billings KS, Ohashi T, Allen MD, Best RB, Randles LG, Erickson HP, Clarke J (2007) Designing an extracellular matrix protein with enhanced mechanical stability. Proc Natl Acad Sci USA 104(23):9633–9637. doi:10.1073/pnas.0609901104
62. Rakshit S, Zhang Y, Manibog K, Shafraz O, Sivasankar S (2012) Ideal, catch, and slip bonds in cadherin adhesion. Proc Natl Acad Sci 109(46):18815–18820. doi:10.1073/pnas.1208349109
63. Rico F, Chu C, Abdulreda MH, Qin Y, Moy VT (2010) Temperature modulation of integrin-mediated cell adhesion. Biophys J 99(5):1387–1396. doi:10.1016/j.bpj.2010.06.037
64. Rico F, Chu C, Moy VT (2011) Force-clamp measurements of receptor–ligand interactions atomic force microscopy in biomedical research. In: Braga PC, Ricci D (eds) Methods in molecular biology, vol 736. Humana Press, New York, pp 331–353. doi:10.1007/978-1-61779-105-5_20
65. Rief M, Pascual J, Saraste M, Gaub HE (1999) Single molecule force spectroscopy of spectrin repeats: low unfolding forces in helix bundles. J Mol Biol 286(2):553–561
66. Thomas WE, Trintchina E, Forero M, Vogel V, Sokurenko EV (2002) Bacterial adhesion to target cells enhanced by shear force. Cell 109(7):913–923
67. Thomas WE, Vogel V, Sokurenko E (2008) Biophysics of catch bonds. Annu Rev Biophys 37(1):399–416. doi:10.1146/annurev.biophys.37.032807.125804
68. van Roy F, Berx G (2008) The cell-cell adhesion molecule E-cadherin. Cell Mol Life Sci 65(23):3756–3788. doi:10.1007/s00018-008-8281-1
69. Vogel V (2006) Mechanotransduction involving multimodular proteins: converting force into biochemical signals. Annu Rev Biophys Biomol Struct 35:459–488. doi:10.1146/annurev.biophys.35.040405.102013
70. Wojcikiewicz EP, Abdulreda MH, Zhang X, Moy VT (2006) Force spectroscopy of LFA-1 and its ligands, ICAM-1 and ICAM-2. Biomacromolecules 7(11):3188–3195. doi:10.1021/bm060559c
71. Erickson HP (1994) Reversible unfolding of fibronectin type-III and immunoglobulin domains provides the structural basis for stretch and elasticity of titin and fibronectin. Proc Natl Acad Sci USA 91:10114–10118
72. Erickson HP (1997) Stretching single protein molecules: titin is a weird spring. Science 276(5315):1090–1092. doi:10.1126/science.276.5315.1090
73. Rief M, Oesterhelt F, Heymann B, Gaub HE (1997) Single molecule force spectroscopy on polysaccharides by atomic force microscopy. Science 275(5304):1295–1297. doi:10.1126/science.275.5304.1295
74. Kellermayer MSZ, Smith SB, Granzier HL, Bustamante C (1997) Folding-unfolding transitions in single titin molecules characterized with laser tweezers. Science 276(5315):1112–1116
75. Li HB, Linke WA, Oberhauser AF, Carrion-Vazquez M, Kerkviliet JG, Lu H, Marszalek PE, Fernandez JM (2002) Reverse engineering of the giant muscle protein titin. Nature 418(6901):998–1002
76. Tskhovrebova L, Trinick J, Sleep JA, Simmons RM (1997) Elasticity and unfolding of single molecules of the giant muscle protein titin. Nature 387(6630):308–312

77. Davies GJ, Mackenzie L, Varrot A, Dauter M, Brzozowski AM, Schülein M, Withers SG (1998) Snapshots along an enzymatic reaction coordinate: analysis of a retaining β-glycoside hydrolase. Biochemistry 37(34):11707–11713. doi:10.1021/bi981315i
78. Kim IL, Mauck RL, Burdick JA (2011) Hydrogel design for cartilage tissue engineering: a case study with hyaluronic acid. Biomaterials 32(34):8771–8782. doi:10.1016/j.biomaterials.2011.08.073
79. Hills BA (2000) Boundary lubrication in vivo. Proc Inst Mech Eng H 214(1):83–94. doi:10.1243/0954411001535264
80. Hui AY, McCarty WJ, Masuda K, Firestein GS, Sah RL (2012) A systems biology approach to synovial joint lubrication in health, injury, and disease. Wiley Interdiscip Rev Syst Biol Med 4(1):15–37. doi:10.1002/wsbm.157
81. Coles JM, Chang DP, Zauscher S (2010) Molecular mechanisms of aqueous boundary lubrication by mucinous glycoproteins. Curr Opin Colloid Interface Sci 15(6):406–416. doi:10.1016/j.cocis.2010.07.002
82. Fisher TE, Marszalek PE, Fernandez JM (2000) Stretching single molecules into novel conformations using the atomic force microscope. Nat Struct Mol Biol 7(9):719–724
83. Marszalek PE, Dufrene YF (2012) Stretching single polysaccharides and proteins using atomic force microscopy. Chem Soc Rev 41(9):3523–3534. doi:10.1039/c2cs15329g
84. Puchner EM, Gaub HE (2009) Force and function: probing proteins with AFM-based force spectroscopy. Curr Opin Struct Biol 19(5):605–614. doi:S0959-440X(09)00135-3 [pii], doi:10.1016/j.sbi.2009.09.005
85. Dufrene YF, Evans E, Engel A, Helenius J, Gaub HE, Muller DJ (2011) Five challenges to bringing single-molecule force spectroscopy into living cells. Nat Meth 8(2):123–127
86. Muller DJ, Dufrene YF (2008) Atomic force microscopy as a multifunctional molecular toolbox in nanobiotechnology. Nat Nanotechnol 3(5):261–269. doi:10.1038/nnano.2008.100
87. Muller DJ, Helenius J, Alsteens D, Dufrene YF (2009) Force probing surfaces of living cells to molecular resolution. Nat Chem Biol 5(6):383–390. doi:10.1038/nchembio.181
88. Hansma PK (2006) Molecular mechanics of single molecules. Structure 14(3):390–391
89. Viani MB, Schaffer TE, Paloczi GT, Pietrasanta LI, Smith BL, Thompson JB, Richter M, Rief M, Gaub HE, Plaxco KW, Cleland AN, Hansma HG, Hansma PK (1999) Fast imaging and fast force spectroscopy of single biopolymers with a new atomic force microscope designed for small cantilevers. Rev Sci Instrum 70(11):4300–4303
90. Rabbi M, Marszalek P (2008) Probing polysaccharide and protein mechanics by atomic force microscopy. In: Selvin PR, Ha T (eds) Single-molecule techniques: a laboratory manual. Cold Spring Harbor Laboratory Press, Cold Spring Harbor, pp 371–394
91. Flory PJ (1953) Principles of polymer chemistry. Cornell University Press, Ithaca
92. Flory PJ (1989) Statistical Mechanics of Chain Molecules. Hanser Publishers, New York
93. Bustamante C, Marko JF, Siggia ED, Smith S (1994) Entropic elasticity of lambda-phage dna. Science 265(5178):1599–1600
94. Smith SB, Finzi L, Bustamante C (1992) Direct mechanical measurements of the elasticity of single DNA-molecules by using magnetic beads. Science 258(5085):1122–1126
95. Bustamante C (1994) Entropic elasticity of [lambda]-phage DNA. Science 265:1599–1600
96. Smith SB, Cui YJ, Bustamante C (1996) Overstretching B-DNA: the elastic response of individual double-stranded and single-stranded DNA molecules. Science 271(5250):795–799
97. Marszalek PE, Lu H, Li HB, Carrion-Vazquez M, Oberhauser AF, Schulten K, Fernandez JM (1999) Mechanical unfolding intermediates in titin modules. Nature 402(6757):100–103
98. Marszalek PE, Oberhauser AF, Pang YP, Fernandez JM (1998) Polysaccharide elasticity governed by chair-boat transitions of the glucopyranose ring. Nature 396(6712):661–664
99. Strick TR, Dessinges MN, Charvin G, Dekker NH, Allemand JF, Bensimon D, Croquette V (2003) Stretching of macromolecules and proteins. Rep Prog Phys 66(1):1–45
100. Frentrup H, Allen MS (2011) Error in dynamic spring constant calibration of atomic force microscope probes due to nonuniform cantilevers. Nanotechnology 22(29):295703

101. Burnham N, Chen X, Hodges C, Matei G, Thoreson E, Roberts C, Davies M, Tendler S (2003) Comparison of calibration methods for atomic-force microscopy cantilevers. Nanotechnology 14(1):1
102. Binnig G, Quate CF, Gerber C (1986) Atomic force microscope. Phys Rev Lett 56(9):930–933
103. Rugar D, Hansma P (1990) Atomic force microscopy. Physics Today 43(10):23–30
104. Binnig G, Rohrer H, Gerber C, Weibel E (1982) Tunneling through a controllable vacuum gap. Appl Phys Lett 40(2):178–180
105. Binnig G, Rohrer H, Gerber C, Weibel E (1983) 7x7 reconstruction on Si(111) resolved in real space. Phys Rev Lett 50(2):120–123
106. Hansma P, Elings V, Marti O, Bracker C (1988) Scanning tunneling microscopy and atomic force microscopy: application to biology and technology. Science 242:209–216
107. Oberhauser AF, Hansma PK, Carrion-Vazquez M, Fernandez JM (2001) Stepwise unfolding of titin under force-clamp atomic force microscopy. Proc Natl Acad Sci USA 98(2):468–472
108. Moffitt JR, Chemla YR, Smith SB, Bustamante C (2008) Recent advances in optical tweezers. Annu Rev Biochem 77:205–228. doi:10.1146/annurev.biochem.77.043007.090225
109. Visscher K, Block SM (1998) Versatile optical traps with feedback control. Molecular Motors and the Cytoskeleton, Pt B 298:460–489
110. Mehta AD, Rief M, Spudich JA, Smith DA, Simmons RM (1999) Single-molecule biomechanics with optical methods. Science 283(5408):1689–1695
111. Moffitt JR, Chemla YR, Izhaky D, Bustamante C (2006) Differential detection of dual traps improves the spatial resolution of optical tweezers. PNAS 103(24):9006–9011. doi:10.1073/pnas.0603342103
112. Ashkin A (1970) Acceleration and trapping of particles by radiation pressure. Phys Rev Lett 24(4):156–159. doi:10.1103/PhysRevLett.24.156
113. De Vlaminck I, Dekker C (2012) Recent advances in magnetic tweezers. Annu Rev Biophys 41:453–472
114. Lipfert J, Kerssemakers JWJ, Jager T, Dekker NH (2010) Magnetic torque tweezers: measuring torsional stiffness in DNA and RecA-DNA filaments. Nat Methods 7(12):977–980. doi:10.1038/nmeth.1520
115. Lipfert J, Hao XM, Dekker NH (2009) Quantitative modeling and optimization of magnetic tweezers. Biophys J 96(12):5040–5049. doi:10.1016/j.bpj.2009.03.055
116. Strick T, Allemand JF, Croquette V, Bensimon D (2000) Twisting and stretching single DNA molecules. Prog Biophys Mol Biol 74(1–2):115–140. doi:10.1016/s0079-6107(00)00018-3
117. Strick TR, Allemand JF, Bensimon D, Bensimon A, Croquette V (1996) The elasticity of a single supercoiled DNA molecule. Science 271(5257):1835–1837
118. Strick TR, Allemand JF, Bensimon D, Croquette V (1998) Behavior of supercoiled DNA. Biophys J 74(4):2016–2028
119. Simson DA, Ziemann F, Strigl M, Merkel R (1998) Micropipet-based pico force transducer: in depth analysis and experimental verification. Biophys J 74(4):2080–2088
120. Deamer DW, Akeson M (2000) Nanopores and nucleic acids: prospects for ultrarapid sequencing. Trends Biotechnol 18(4):147–151. doi:10.1016/S0167-7799(00)01426-8
121. Kasianowicz JJ, Brandin E, Branton D, Deamer DW (1996) Characterization of individual polynucleotide molecules using a membrane channel. Proc Natl Acad Sci 93(24):13770–13773
122. Dekker C (2007) Solid-state nanopores. Nat Nanotechnol 2(4):209–215. doi:10.1038/nnano.2007.27
123. Rodriguez-Larrea D, Bayley H (2013) Multistep protein unfolding during nanopore translocation. Nat Nanotechnol 8(4):288–295. doi:10.1038/nnano.2013.22
124. Dudko OK, Mathé J, Meller A (2010) Chapter twenty-one – nanopore force spectroscopy tools for analyzing single biomolecular complexes. In: Nils GW (ed) Methods in enzymology, vol 475. Academic Press, New York, pp 565–589. doi:10.1016/S0076-6879(10)75021-7

125. Perkins TT, Smith DE, Chu S (1997) Single polymer dynamics in an elongational flow. Science 276(5321):2016–2021
126. Perkins TT, Smith DE, Larson RG, Chu S (1995) Stretching of a single tethered polymer in a uniform-flow. Science 268(5207):83–87. doi:10.1126/science.7701345
127. Davenport RJ, Wuite GJL, Landick R, Bustamante C (2000) Single-molecule study of transcriptional pausing and arrest by E-coli RNA polymerase. Science 287(5462):2497–2500. doi:10.1126/science.287.5462.2497
128. Kim SJ, Blainey PC, Schroeder CM, Xie XS (2007) Multiplexed single-molecule assay for enzymatic activity on flow-stretched DNA. Nat Methods 4(5):397–399. doi:10.1038/nmeth1037
129. Schafer DA, Gelles J, Sheetz MP, Landick R (1991) Transcription by single molecules of RNA polymerase observed by light microscopy. Nature 352(6334):444–448. doi:10.1038/352444a0
130. Yin H, Landick R, Gelles J (1994) Tethered particle motion method for studying transcript elongation by a single RNA polymerase molecule. Biophys J 67(6):2468–2478. doi:10.1016/S0006-3495(94)80735-0
131. Finzi L, Gelles J (1995) Measurement of lactose repressor-mediated loop formation and breakdown in single DNA molecules. Science 267(5196):378–380
132. van den Broek B, Vanzi F, Normanno D, Pavone FS, Wuite GJ (2006) Real-time observation of DNA looping dynamics of Type IIE restriction enzymes NaeI and NarI. Nucleic Acids Res 34(1):167–174. doi:10.1093/nar/gkj432
133. Vanzi F, Broggio C, Sacconi L, Pavone FS (2006) Lac repressor hinge flexibility and DNA looping: single molecule kinetics by tethered particle motion. Nucleic Acids Res 34(12):3409–3420. doi:10.1093/nar/gkl393
134. Wong OK, Guthold M, Erie DA, Gelles J (2008) Interconvertible lac repressor-DNA loops revealed by single-molecule experiments. PLoS Biol 6(9):e232. doi:10.1371/journal.pbio.0060232
135. Han L, Garcia HG, Blumberg S, Towles KB, Beausang JF, Nelson PC, Phillips R (2009) Concentration and length dependence of DNA looping in transcriptional regulation. PLoS One 4(5):e5621. doi:10.1371/journal.pone.0005621
136. Rutkauskas D, Zhan H, Matthews KS, Pavone FS, Vanzi F (2009) Tetramer opening in LacI-mediated DNA looping. Proc Natl Acad Sci USA 106(39):16627–16632. doi:10.1073/pnas.0904617106
137. Zurla C, Manzo C, Dunlap D, Lewis DE, Adhya S, Finzi L (2009) Direct demonstration and quantification of long-range DNA looping by the lambda bacteriophage repressor. Nucleic Acids Res 37(9):2789–2795. doi:10.1093/nar/gkp134
138. Chen YF, Milstein JN, Meiners JC (2010) Protein-mediated DNA loop formation and breakdown in a fluctuating environment. Phys Rev Lett 104(25):258103
139. Chen Y-F, Milstein J, Meiners J-C (2010) Femtonewton entropic forces can control the formation of protein-mediated DNA loops. Phys Rev Lett 104(4):048301
140. Johnson S, Linden M, Phillips R (2012) Sequence dependence of transcription factor-mediated DNA looping. Nucleic Acids Res 40(16):7728–7738. doi:10.1093/nar/gks473
141. Laurens N, Rusling DA, Pernstich C, Brouwer I, Halford SE, Wuite GJ (2012) DNA looping by FokI: the impact of twisting and bending rigidity on protein-induced looping dynamics. Nucleic Acids Res 40(11):4988–4997. doi:10.1093/nar/gks184
142. Manzo C, Zurla C, Dunlap DD, Finzi L (2012) The effect of nonspecific binding of lambda repressor on DNA looping dynamics. Biophys J 103(8):1753–1761. doi:10.1016/j.bpj.2012.09.006
143. Pouget N, Turlan C, Destainville N, Salomé L, Chandler M (2006) IS911 transpososome assembly as analysed by tethered particle motion. Nucleic Acids Res 34(16):4313–4323
144. Tolic-Norrelykke SF, Rasmussen MB, Pavone FS, Berg-Sorensen K, Oddershede LB (2006) Stepwise bending of DNA by a single TATA-box binding protein. Biophys J 90(10):3694–3703. doi:10.1529/biophysj.105.074856

145. Mumm JP, Landy A, Gelles J (2006) Viewing single lambda site-specific recombination events from start to finish. EMBO J 25(19):4586–4595. doi:10.1038/sj.emboj.7601325
146. Fan HF (2012) Real-time single-molecule tethered particle motion experiments reveal the kinetics and mechanisms of Cre-mediated site-specific recombination. Nucleic Acids Res 40(13):6208–6222. doi:10.1093/nar/gks274
147. Monico C, Capitanio M, Belcastro G, Vanzi F, Pavone FS (2013) Optical methods to study protein-DNA interactions in vitro and in living cells at the single-molecule level. Int J Mol Sci 14(2):3961–3992
148. Vanzi F, Sacconi L, Pavone FS (2007) Analysis of kinetics in noisy systems: application to single molecule tethered particle motion. Biophys J 93(1):21–36. doi:10.1529/biophysj.106.094151
149. Segall DE, Nelson PC, Phillips R (2006) Volume-exclusion effects in tethered-particle experiments: bead size matters. Phys Rev Lett 96(8):088306
150. Milstein JN, Chen YF, Meiners JC (2011) Bead size effects on protein-mediated DNA looping in tethered-particle motion experiments. Biopolymers 95(2):144–150. doi:10.1002/bip.21547
151. Fan H-F, Li H-W (2009) Studying RecBCD Helicase translocation along Ç-DNA using tethered particle motion with a stretching force. Biophys J 96(5):1875–1883
152. Plenat T, Tardin C, Rousseau P, Salome L (2012) High-throughput single-molecule analysis of DNA-protein interactions by tethered particle motion. Nucleic Acids Res 40(12):e89. doi:10.1093/nar/gks250
153. Beausang JF, Zurla C, Manzo C, Dunlap D, Finzi L, Nelson PC (2007) DNA looping kinetics analyzed using diffusive hidden Markov model. Biophys J 92(8):L64–L66
154. Manzo C, Finzi L (2010) Quantitative analysis of DNA-looping kinetics from tethered particle motion experiments. Methods Enzymol 475:199–220. doi:10.1016/S0076-6879(10)75009-6
155. Bustamante C, Macosko JC, Wuite GJL (2000) Grabbing the cat by the tail: manipulating molecules one by one. Nat Rev Mol Cell Biol 1(2):130–136
156. Neuman KC, Nagy A (2008) Single-molecule force spectroscopy: optical tweezers, magnetic tweezers and atomic force microscopy. Nat Methods 5(6):491–505. doi:10.1038/nmeth.1218
157. Giannotti MI, Vancso GJ (2007) Interrogation of single synthetic polymer chains and polysaccharides by AFM-based force spectroscopy. Chemphyschem 8(16):2290–2307. doi:10.1002/cphc.200700175
158. Greenleaf WJ, Woodside MT, Block SM (2007) High-resolution, single-molecule measurements of biomolecular motion. Annu Rev Biophys Biomol Struct 36(1):171–190. doi:10.1146/annurev.biophys.36.101106.101451
159. Tinoco I, Li PTX, Bustamante C (2006) Determination of thermodynamics and kinetics of RNA reactions by force. Quart Rev Biophys 39(4):325–360. doi:10.1017/S0033583506004446
160. Dufrêne Y, Hinterdorfer P (2008) Recent progress in AFM molecular recognition studies. Pflügers Arch 456(1):237–245. doi:10.1007/s00424-007-0413-1
161. Moy VT, Florin EL, Gaub HE (1994) Adhesive forces between ligand and receptor measured by Afm. Colloid Surf A-Physicochem Eng 93:343–348
162. Wuite GJL, Smith SB, Young M, Keller D, Bustamante C (2000) Single-molecule studies of the effect of template tension on T7 DNA polymerase activity. Nature 404(6773):103–106
163. Onoa B, Dumont S, Liphardt J, Smith SB, Tinoco I, Bustamante C (2003) Identifying kinetic barriers to mechanical unfolding of the T-thermophila ribozyme. Science 299(5614):1892–1895
164. Stigler J, Ziegler F, Gieseke A, Gebhardt JCM, Rief M (2011) The complex folding network of single calmodulin molecules. Science 334(6055):512–516. doi:10.1126/science.1207598
165. Koster DA, Croquette V, Dekker C, Shuman S, Dekker NH (2005) Friction and torque govern the relaxation of DNA supercoils by eukaryotic topoisomerase IB. Nature 434(7033):671–674. doi:10.1038/nature03395

166. Gore J, Bryant Z, Stone MD, Nollmann MN, Cozzarelli NR, Bustamante C (2006) Mechanochemical analysis of DNA gyrase using rotor bead tracking. Nature 439(7072):100–104
167. Merkel R, Nassoy P, Leung A, Ritchie K, Evans E (1999) Energy landscapes of receptor-ligand bonds explored with dynamic force spectroscopy. Nature 397(6714):50–53. doi:10.1038/16219
168. Dudko OK, Mathe J, Szabo A, Meller A, Hummer G (2007) Extracting kinetics from single-molecule force spectroscopy: nanopore unzipping of DNA hairpins. Biophys J 92(12):4188–4195. doi:10.1529/biophysj.106.102855
169. Hutter JL, Bechhoefer J (1993) Calibration of atomic-force microscope tips. Rev Sci Instrum 64:1868
170. Hinterdorfer P, Dufrêne YF (2006) Detection and localization of single molecular recognition events using atomic force microscopy. Nat Methods 3(5):347–355
171. Taniguchi Y, Kawakami M (2010) Application of HaloTag protein to covalent immobilization of recombinant proteins for single molecule force spectroscopy. Langmuir 26(13):10433–10436
172. Wong J, Chilkoti A, Moy VT (1999) Direct force measurements of the streptavidin–biotin interaction. Biomol Eng 16(1):45–55
173. Kienberger F, Kada G, Gruber HJ, Pastushenko VP, Riener C, Trieb M, Knaus HG, Schindler H, Hinterdorfer P (2000) Recognition force spectroscopy studies of the NTA-His6 bond. Single Molecules 1(1):59–65
174. Bustamante C, Marko J, Siggia E, Smith S (1994) Entropic elasticity of lambda-phage DNA. Science 265:1599–1601
175. Merkel R, Nassoy P, Leung A, Ritchie K, Evans E (1999) Energy landscapes of receptor–ligand bonds explored with dynamic force spectroscopy. Nature 397(6714):50–53
176. Brockwell DJ, Paci E, Zinober RC, Beddard GS, Olmsted PD, Smith DA, Perham RN, Radford SE (2003) Pulling geometry defines the mechanical resistance of a beta-sheet protein. Nat Struct Biol 10(9):731–737. doi:10.1038/nsb968
177. Dietz H, Rief M (2006) Protein structure by mechanical triangulation. Proc Natl Acad Sci USA 103(5):1244–1247
178. Lee W, Zeng X, Zhou H-X, Bennett V, Yang W, Marszalek PE (2010) Full reconstruction of a vectorial protein folding pathway by atomic force microscopy and molecular dynamics simulations. J Biol Chem 285(49):38167–38172. doi:10.1074/jbc.M110.179697
179. Li L, Wetzel S, Pluckthun A, Fernandez JM (2006) Stepwise unfolding of ankyrin repeats in a single protein revealed by atomic force microscopy. Biophys J 90(4):L30–L32. doi:10.1529/biophysj.105.078436
180. Lee G, Abdi K, Jiang Y, Michaely P, Bennett V, Marszalek PE (2006) Nanospring behaviour of ankyrin repeats. Nature 440(7081):246–249. doi:nature04437 [pii]. doi:10.1038/nature04437
181. Merz T, Wetzel SK, Firbank S, Pluckthun A, Grutter MG, Mittl PR (2008) Stabilizing ionic interactions in a full-consensus ankyrin repeat protein. J Mol Biol 376(1):232–240. doi:10.1016/j.jmb.2007.11.047
182. Kim M, Abdi K, Lee G, Rabbi M, Lee W, Yang M, Schofield CJ, Bennett V, Marszalek PE (2010) Fast and forceful refolding of stretched alpha-helical solenoid proteins. Biophys J 98(12):3086–3092. doi:10.1016/j.bpj.2010.02.054
183. Valbuena A, Vera Andrés M, Oroz J, Menéndez M, Carrión-Vázquez M (2012) Mechanical properties of β-catenin revealed by single-molecule experiments. Biophys J 103(8):1744–1752. doi:10.1016/j.bpj.2012.07.051
184. Xing Y, Takemaru K, Liu J, Berndt JD, Zheng JJ, Moon RT, Xu W (2008) Crystal structure of a full-length beta-catenin. Structure 16(3):478–487. doi:10.1016/j.str.2007.12.021
185. Best RB, Li B, Steward A, Daggett V, Clarke J (2001) Can non-mechanical proteins withstand force? Stretching barnase by atomic force microscopy and molecular dynamics simulation. Biophys J 81(4):2344–2356. doi:10.1016/S0006-3495(01)75881-X
186. Martin C, Richard V, Salem M, Hartley R, Mauguen Y (1999) Refinement and structural analysis of barnase at 1.5 A resolution. Acta Crystallogr D Biol Crystallogr 55(Pt 2):386–398

187. Junker JP, Ziegler F, Rief M (2009) Ligand-dependent equilibrium fluctuations of single calmodulin molecules. Science 323(5914):633–637. doi:10.1126/science.1166191
188. Chattopadhyaya R, Meador WE, Means AR, Quiocho FA (1992) Calmodulin structure refined at 1.7 Å resolution. J Mol Biol 228(4):1177–1192
189. Hoffmann T, Tych KM, Brockwell DJ, Dougan L (2013) Single-molecule force spectroscopy identifies a small cold shock protein as being mechanically robust. J Phys Chem B 117(6):1819–1826. doi:10.1021/jp310442s
190. Kremer W, Schuler B, Harrieder S, Geyer M, Gronwald W, Welker C, Jaenicke R, Kalbitzer HR (2001) Solution NMR structure of the cold-shock protein from the hyperthermophilic bacterium *Thermotoga maritima*. Eur J Biochem 268(9):2527–2539
191. Ainavarapu SRK, Li L, Badilla CL, Fernandez JM (2005) Ligand binding modulates the mechanical stability of dihydrofolate reductase. Biophys J 89(5):3337–3344
192. Lewis WS, Cody V, Galitsky N, Luft JR, Pangborn W, Chunduru SK, Spencer HT, Appleman JR, Blakley RL (1995) Methotrexate-resistant variants of human dihydrofolate reductase with substitutions of leucine 22 Kinetics, crystallography, and potential as selectable markers. J Biol Chem 270(10):5057–5064
193. Tang L, Whittingham JL, Verma CS, Caves LS, Dodson GG (1999) Structural consequences of the B5 histidine –> tyrosine mutation in human insulin characterized by X-ray crystallography and conformational analysis. Biochemistry 38(37):12041–12051
194. Perez-Jimenez R, Garcia-Manyes S, Ainavarapu SRK, Fernandez JM (2006) Mechanical unfolding pathways of the enhanced yellow fluorescent protein revealed by single molecule force spectroscopy. J Biol Chem 281(52):40010–40014
195. Wachter RM, Elsliger MA, Kallio K, Hanson GT, Remington SJ (1998) Structural basis of spectral shifts in the yellow-emission variants of green fluorescent protein. Structure 6(10):1267–1277
196. Brown André E, Litvinov RI, Discher DE, Weisel JW (2007) Forced unfolding of coiled-coils in fibrinogen by single-molecule AFM. Biophys J 92(5):L39–L41
197. Cao Y, Lam C, Wang M, Li H (2006) Nonmechanical protein can have significant mechanical stability. Angew Chem 118(4):658–661
198. Cao Y, Li H (2007) Polyprotein of GB1 is an ideal artificial elastomeric protein. Nat Mater 6(2):109–114
199. Nieuwkoop AJ, Wylie BJ, Franks WT, Shah GJ, Rienstra CM (2009) Atomic resolution protein structure determination by three-dimensional transferred echo double resonance solid-state nuclear magnetic resonance spectroscopy. J Chem Phys 131(9):095101. doi:10.1063/1.3211103
200. Cao Y, Yoo T, Li H (2008) Single molecule force spectroscopy reveals engineered metal chelation is a general approach to enhance mechanical stability of proteins. Proc Natl Acad Sci 105(32):11152–11157
201. Abu-Lail NI, Ohashi T, Clark RL, Erickson HP, Zauscher S (2006) Understanding the elasticity of fibronectin fibrils: unfolding strengths of FN-III and GFP domains measured by single molecule force spectroscopy. Matrix Biol 25(3):175–184
202. Dietz H, Rief M (2004) Exploring the energy landscape of GFP by single-molecule mechanical experiments. Proc Natl Acad Sci USA 101(46):16192–16197
203. Battistutta R, Negro A, Zanotti G (2000) Crystal structure and refolding properties of the mutant F99S/M153T/V163A of the green fluorescent protein. Proteins 41(4):429–437
204. Newman J, Peat TS, Richard R, Kan L, Swanson PE, Affholter JA, Holmes IH, Schindler JF, Unkefer CJ, Terwilliger TC (1999) Haloalkane dehalogenases: structure of a Rhodococcus enzyme. Biochemistry 38(49):16105–16114
205. Ybe JA, Brodsky FM, Hofmann K, Lin K, Liu SH, Chen L, Earnest TN, Fletterick RJ, Hwang PK (1999) Clathrin self-assembly is mediated by a tandemly repeated superhelix. Nature 399(6734):371–375. doi:10.1038/20708
206. Schwaiger I, Kardinal A, Schleicher M, Noegel AA, Rief M (2003) A mechanical unfolding intermediate in an actin-crosslinking protein. Nat Struct Mol Biol 11(1):81–85

207. Schwaiger I, Schleicher M, Noegel AA, Rief M (2004) The folding pathway of a fast-folding immunoglobulin domain revealed by single-molecule mechanical experiments. EMBO Rep 6(1):46–51
208. Bullard B, Garcia T, Benes V, Leake MC, Linke WA, Oberhauser AF (2006) The molecular elasticity of the insect flight muscle proteins projectin and kettin. Proc Natl Acad Sci USA 103(12):4451–4456
209. Johnson RJ, McCoy JG, Bingman CA, Phillips GN Jr, Raines RT (2007) Inhibition of human pancreatic ribonuclease by the human ribonuclease inhibitor protein. J Mol Biol 368(2):434–449. doi:10.1016/j.jmb.2007.02.005
210. Bornschlögl T, Rief M (2006) Single molecule unzipping of coiled coils: sequence resolved stability profiles. Phys Rev Lett 96(11):118102
211. Bertz M, Rief M (2008) Mechanical unfoldons as building blocks of maltose-binding protein. J Mol Biol 378(2):447–458
212. Quiocho FA, Spurlino JC, Rodseth LE (1997) Extensive features of tight oligosaccharide binding revealed in high-resolution structures of the maltodextrin transport/chemosensory receptor. Structure 5(8):997–1015
213. Berkemeier F, Bertz M, Xiao S, Pinotsis N, Wilmanns M, Grater F, Rief M (2011) Fast-folding alpha-helices as reversible strain absorbers in the muscle protein myomesin. Proc Natl Acad Sci USA 108(34):14139–14144. doi:10.1073/pnas.1105734108
214. Pinotsis N, Lange S, Perriard JC, Svergun DI, Wilmanns M (2008) Molecular basis of the C-terminal tail-to-tail assembly of the sarcomeric filament protein myomesin. EMBO J 27(1):253–264. doi:10.1038/sj.emboj.7601944
215. Schwaiger I, Sattler C, Hostetter DR, Rief M (2002) The myosin coiled-coil is a truly elastic protein structure. Nat Mater 1(4):232–235. doi:10.1038/nmat776
216. Kaiser CM, Bujalowski PJ, Ma L, Anderson J, Epstein HF, Oberhauser AF (2012) Tracking UNC-45 chaperone-myosin interaction with a titin mechanical reporter. Biophys J 102(9):2212–2219
217. Yadavalli VK, Forbes JG, Wang K (2009) Nanomechanics of full-length nebulin: an elastic strain gauge in the skeletal muscle sarcomere. Langmuir 25(13):7496–7505. doi:10.1021/la9009898
218. Cao Y, Kuske R, Li H (2008) Direct observation of Markovian behavior of the mechanical unfolding of individual proteins. Biophys J 95(2):782–788
219. Nauli S, Kuhlman B, Le Trong I, Stenkamp RE, Teller D, Baker D (2002) Crystal structures and increased stabilization of the protein G variants with switched folding pathways NuG1 and NuG2. Protein Sci 11(12):2924–2931
220. Ma L, Xu M, Forman JR, Clarke J, Oberhauser AF (2009) Naturally occurring mutations alter the stability of polycystin-1 polycystic kidney disease (PKD) domains. J Biol Chem 284(47):32942–32949
221. Bycroft M, Bateman A, Clarke J, Hamill SJ, Sandford R, Thomas RL, Chothia C (1999) The structure of a PKD domain from polycystin-1: implications for polycystic kidney disease. EMBO J 18(2):297–305
222. Brockwell DJ, Beddard GS, Paci E, West DK, Olmsted PD, Smith DA, Radford SE (2005) Mechanically unfolding the small, topologically simple protein L. Biophys J 89(1):506
223. O'Neill JW, Kim DE, Baker D, Zhang KY (2001) Structures of the B1 domain of protein L from Peptostreptococcus magnus with a tyrosine to tryptophan substitution. Acta Crystallogr D Biol Crystallogr 57(Pt 4):480–487
224. Valbuena A, Oroz J, Hervás R, Vera AM, Rodríguez D, Menéndez M, Sulkowska JI, Cieplak M, Carrión-Vázquez M (2009) On the remarkable mechanostability of scaffoldins and the mechanical clamp motif. Proc Natl Acad Sci 106(33):13791–13796
225. Spinelli S, Fierobe HP, Belaich A, Belaich JP, Henrissat B, Cambillau C (2000) Crystal structure of a cohesin module from *Clostridium cellulolyticum*: implications for dockerin recognition. J Mol Biol 304(2):189–200. doi:10.1006/jmbi.2000.4191

226. Shimon LJ, Bayer EA, Morag E, Lamed R, Yaron S, Shoham Y, Frolow F (1997) A cohesin domain from *Clostridium thermocellum*: the crystal structure provides new insights into cellulosome assembly. Structure 5(3):381–390
227. Tavares GA, Béguin P, Alzari PM (1997) The crystal structure of a type I cohesin domain at 1.7 Å resolution. J Mol Biol 273(3):701–713
228. Alegre-Cebollada J, Badilla CL, Fernández JM (2010) Isopeptide bonds block the mechanical extension of pili in pathogenic *Streptococcus pyogenes*. J Biol Chem 285(15):11235–11242
229. Kang HJ, Coulibaly F, Clow F, Proft T, Baker EN (2007) Stabilizing isopeptide bonds revealed in gram-positive bacterial pilus structure. Science 318(5856):1625–1628
230. Wang C-C, Tsong T-Y, Hsu Y-H, Marszalek PE (2011) Inhibitor binding increases the mechanical stability of *Staphylococcal Nuclease*. Biophys J 100(4):1094–1099. doi:10.1016/j.bpj.2011.01.011
231. Cotton FA, Hazen EE, Legg MJ (1979) *Staphylococcal nuclease*: proposed mechanism of action based on structure of enzyme—thymidine 3′, 5′-bisphosphate—calcium ion complex at 1.5-Å resolution. Proc Natl Acad Sci 76(6):2551–2555
232. Kotamarthi HC, Sharma R, Koti Ainavarapu SR (2013) Single-molecule studies on PolySUMO proteins reveal their mechanical flexibility. Biophys J 104(10):2273–2281
233. Bayer P, Arndt A, Metzger S, Mahajan R, Melchior F, Jaenicke R, Becker J (1998) Structure determination of the small ubiquitin-related modifier SUMO-1. J Mol Biol 280(2):275–286
234. Huang WC, Ko TP, Li SSL, Wang AHJ (2004) Crystal structures of the human SUMO-2 protein at 1.6 Å and 1.2 Å resolution. Eur J Biochem 271(20):4114–4122
235. Randles LG, Rounsevell RWS, Clarke J (2007) Spectrin domains lose cooperativity in forced unfolding. Biophys J 92(2):571–577. doi:10.1529/biophysj.106.093690
236. Law R, Carl P, Harper S, Dalhaimer P, Speicher DW, Discher DE (2003) Cooperativity in forced unfolding of tandem spectrin repeats. Biophys J 84(1):533–544
237. Kusunoki H, MacDonald RI, Mondragón A (2004) Structural insights into the stability and flexibility of unusual erythroid spectrin repeats. Structure 12(4):645–656
238. Fuson KL, Ma L, Sutton RB, Oberhauser AF (2009) The c2 domains of human synaptotagmin 1 have distinct mechanical properties. Biophys J 96(3):1083–1090
239. Fuson KL, Montes M, Robert JJ, Sutton RB (2007) Structure of human synaptotagmin 1 C2AB in the absence of Ca2+ reveals a novel domain association. Biochemistry 46(45):13041–13048
240. Peng Q, Li H (2008) Atomic force microscopy reveals parallel mechanical unfolding pathways of T4 lysozyme: evidence for a kinetic partitioning mechanism. Proc Natl Acad Sci 105(6):1885–1890
241. Nicholson H, Anderson D, Dao Pin S, Matthews B (1991) Analysis of the interaction between charged side chains and the. alpha.-helix dipole using designed thermostable mutants of phage T4 lysozyme. Biochemistry 30(41):9816–9828
242. Oberhauser AF, Marszalek PE, Erickson HP, Fernandez JM (1998) The molecular elasticity of the extracellular matrix protein tenascin. Nature 393(6681):181–185
243. Ng SP, Rounsevell RW, Steward A, Geierhaas CD, Williams PM, Paci E, Clarke J (2005) Mechanical unfolding of TNfn3: the unfolding pathway of a fnIII domain probed by protein engineering, AFM and MD simulation. J Mol Biol 350(4):776–789
244. Leahy DJ, Hendrickson WA, Aukhil I, Erickson HP (1992) Structure of a fibronectin type III domain from tenascin phased by MAD analysis of the selenomethionyl protein. Science 258(5084):987–991
245. Carrion-Vazquez M, Oberhauser AF, Fowler SB, Marszalek PE, Broedel SE, Clarke J, Fernandez JM (1999) Mechanical and chemical unfolding of a single protein: a comparison. Proc Natl Acad Sci 96(7):3694–3699
246. Stacklies W, Vega MC, Wilmanns M, Grater F (2009) Mechanical network in titin immunoglobulin from force distribution analysis. PLoS Comput Biol 5(3):e1000306. doi:10.1371/journal.pcbi.1000306

247. Puchner EM, Alexandrovich A, Kho AL, Hensen U, Schäfer LV, Brandmeier B, Gräter F, Grubmüller H, Gaub HE, Gautel M (2008) Mechanoenzymatics of titin kinase. Proc Natl Acad Sci 105(36):13385–13390
248. Mayans O, van der Ven PF, Wilm M, Mues A, Young P, Fürst DO, Wilmanns M, Gautel M (1998) Structural basis for activation of the titin kinase domain during myofibrillogenesis. Nature 395(6705):863–869
249. Greene DN, Garcia T, Sutton RB, Gernert KM, Benian GM, Oberhauser AF (2008) Single-molecule force spectroscopy reveals a stepwise unfolding of *Caenorhabditis elegans* giant protein kinase domains. Biophys J 95(3):1360–1370
250. Kobe B, Heierhorst J, Feil SC, Parker MW, Benian GM, Weiss KR, Kemp BE (1996) Giant protein kinases: domain interactions and structural basis of autoregulation. EMBO J 15(24):6810–6821
251. Sharma D, Perisic O, Peng Q, Cao Y, Lam C, Lu H, Li H (2007) Single-molecule force spectroscopy reveals a mechanically stable protein fold and the rational tuning of its mechanical stability. Proc Natl Acad Sci 104(22):9278–9283
252. Kuhlman B, Dantas G, Ireton GC, Varani G, Stoddard BL, Baker D (2003) Design of a novel globular protein fold with atomic-level accuracy. Science 302(5649):1364–1368
253. Carrion-Vazquez M, Li H, Lu H, Marszalek PE, Oberhauser AF, Fernandez JM (2003) The mechanical stability of ubiquitin is linkage dependent. Nat Struct Mol Biol 10(9):738–743
254. Vijay-Kumar S, Bugg CE, Cook WJ (1987) Structure of ubiquitin refined at 1.8 Å resolution. J Mol Biol 194(3):531–544
255. Isralewitz B, Gao M, Schulten K (2001) Steered molecular dynamics and mechanical functions of proteins. Curr Opin Struct Biol 11(2):224–230
256. Neumann J, Gottschalk K-E (2009) The effect of different force applications on the protein-protein complex barnase-barstar. Biophys J 97(6):1687–1699
257. Gao M, Craig D, Lequin O, Campbell ID, Vogel V, Schulten K (2003) Structure and functional significance of mechanically unfolded fibronectin type III1 intermediates. Proc Natl Acad Sci 100(25):14784–14789
258. Krammer A, Lu H, Isralewitz B, Schulten K, Vogel V (1999) Forced unfolding of the fibronectin type III module reveals a tensile molecular recognition switch. Proc Natl Acad Sci 96(4):1351–1356
259. Lee W, Strümpfer J, Bennett V, Schulten K, Marszalek PE (2012) Mutation of conserved histidines alters tertiary structure and nanomechanics of consensus ankyrin repeats. J Biol Chem 287(23):19115–19121. doi:10.1074/jbc.M112.365569
260. Paramore S, Voth GA (2006) Examining the influence of linkers and tertiary structure in the forced unfolding of multiple-repeat spectrin molecules. Biophys J 91(9):3436–3445
261. Paci E, Karplus M (2000) Unfolding proteins by external forces and temperature: the importance of topology and energetics. Proc Natl Acad Sci USA 97(12):6521–6526
262. Cao Y, Er KS, Parhar R, Li H (2009) A force spectroscopy based single molecule metal binding assay. Chemphyschem 10(9–10):1450–1454
263. Cao Y, Balamurali M, Sharma D, Li H (2007) A functional single-molecule binding assay via force spectroscopy. Proc Natl Acad Sci 104(40):15677–15681
264. Bertz M, Rief M (2009) Ligand binding mechanics of maltose binding protein. J Mol Biol 393(5):1097–1105
265. Krasnoslobodtsev AV, Peng J, Asiago JM, Hindupur J, Rochet J-C, Lyubchenko YL (2012) Effect of spermidine on misfolding and interactions of alpha-synuclein. PLoS One 7(5):e38099
266. Kim B-H, Palermo NY, Lovas S, Zaikova T, Keana JF, Lyubchenko YL (2011) Single-molecule atomic force microscopy force spectroscopy study of Aβ-40 interactions. Biochemistry 50(23):5154–5162
267. Lv Z, Condron MM, Teplow DB, Lyubchenko YL (2013) Nanoprobing of the effect of Cu2+ cations on misfolding, interaction and aggregation of amyloid β peptide. J Neuroimmune Pharmacol 8(1):262–273

268. Schwesinger F, Ros R, Strunz T, Anselmetti D, Güntherodt H-J, Honegger A, Jermutus L, Tiefenauer L, Plückthun A (2000) Unbinding forces of single antibody-antigen complexes correlate with their thermal dissociation rates. Proc Natl Acad Sci 97(18):9972–9977
269. Berquand A, Xia N, Castner DG, Clare BH, Abbott NL, Dupres V, Adriaensen Y, Dufrêne YF (2005) Antigen binding forces of single antilysozyme Fv fragments explored by atomic force microscopy. Langmuir 21(12):5517–5523
270. Kienberger F, Kada G, Mueller H, Hinterdorfer P (2005) Single molecule studies of antibody–antigen interaction strength versus intra-molecular antigen stability. J Mol Biol 347(3):597–606
271. Bonanni B, Kamruzzahan A, Bizzarri A, Rankl C, Gruber H, Hinterdorfer P, Cannistraro S (2005) Single molecule recognition between cytochrome C 551 and gold-immobilized azurin by force spectroscopy. Biophys J 89(4):2783–2791
272. De Paris R, Strunz T, Oroszlan K, Güntherodt H-J, Hegner M (2000) Force spectroscopy and dynamics of the biotin-avidin bond studied by scanning force microscopy. Single Molecules 1(4):285–290
273. Baumgartner W, Hinterdorfer P, Ness W, Raab A, Vestweber D, Schindler H, Drenckhahn D (2000) Cadherin interaction probed by atomic force microscopy. Proc Natl Acad Sci 97(8):4005–4010
274. Leckband D, Sivasankar S (2012) Cadherin recognition and adhesion. Curr Opin Cell Biol 24(5):620–627
275. Bartels FW, Baumgarth B, Anselmetti D, Ros R, Becker A (2003) Specific binding of the regulatory protein ExpG to promoter regions of the galactoglucan biosynthesis gene cluster of *Sinorhizobium meliloti* – a combined molecular biology and force spectroscopy investigation. J Struct Biol 143(2):145–152
276. Hinterdorfer P, Kienberger F, Raab A, Gruber HJ, Baumgartner W, Kada G, Riener C, Wielert-Badt S, Borken C, Schindler H (2000) Poly (ethylene glycol): an ideal spacer for molecular recognition force microscopy/spectroscopy. Single Molecules 1(2):99–103
277. Schmitt L, Ludwig M, Gaub HE, Tampe R (2000) A metal-chelating microscopy tip as a new toolbox for single-molecule experiments by atomic force microscopy. Biophys J 78(6):3275–3285
278. Taranta M, Bizzarri AR, Cannistraro S (2008) Probing the interaction between p53 and the bacterial protein azurin by single molecule force spectroscopy. J Mol Recognit 21(1):63–70
279. Fritz J, Katopodis AG, Kolbinger F, Anselmetti D (1998) Force-mediated kinetics of single P-selectin/ligand complexes observed by atomic force microscopy. Proc Natl Acad Sci 95(21):12283–12288
280. Kim M, Wang CC, Benedetti F, Marszalek PE (2012) A nanoscale force probe for gauging intermolecular interactions. Angew Chem 124(8):1939–1942
281. Tang J, Ebner A, Badelt-Lichtblau H, Völlenkle C, Rankl C, Kraxberger B, Leitner M, Wildling L, Gruber HJ, Sleytr UB (2008) Recognition imaging and highly ordered molecular templating of bacterial S-layer nanoarrays containing affinity-tags. Nano Letters 8(12):4312–4319
282. Garcia-Manyes S, Badilla CL, Alegre-Cebollada J, Javadi Y, Fernández JM (2012) Spontaneous dimerization of titin protein Z1Z2 domains induces strong nanomechanical anchoring. J Biol Chem 287(24):20240–20247. doi:10.1074/jbc.M112.355883
283. Lv S, Dudek DM, Cao Y, Balamurali M, Gosline J, Li H (2010) Designed biomaterials to mimic the mechanical properties of muscles. Nature 465(7294):69–73
284. Cluzel P, Lebrun A, Heller C, Lavery R, Viovy J-L, Chatenay D, Caron F (1996) DNA: an extensible molecule. Science 271:792–794
285. Cocco S, Yan J, Leger J-F, Chatenay D, Marko JF (2004) Overstretching and force-driven strand separation of double-helix DNA. Phys Rev E 70(1):011910
286. Leger J, Romano G, Sarkar A, Robert J, Bourdieu L, Chatenay D, Marko J (1999) Structural transitions of a twisted and stretched DNA molecule. Phys Rev Lett 83(5):1066

287. Strick T, Dessinges M, Charvin G, Dekker N, Allemand J, Bensimon D, Croquette V (2003) Stretching of macromolecules and proteins. Rep Prog Phys 66(1):1
288. van Mameren J, Gross P, Farge G, Hooijman P, Modesti M, Falkenberg M, Wuite GJ, Peterman EJ (2009) Unraveling the structure of DNA during overstretching by using multicolor, single-molecule fluorescence imaging. Proc Natl Acad Sci 106(43):18231–18236
289. Williams MC, Rouzina I, Bloomfield VA (2002) Thermodynamics of DNA interactions from single molecule stretching experiments. Acc Chem Res 35(3):159–166
290. Williams MC, Rouzina I, McCauley MJ (2009) Peeling back the mystery of DNA overstretching. Proc Natl Acad Sci 106(43):18047–18048
291. Williams MC, Wenner JR, Rouzina I, Bloomfield VA (2001) Entropy and heat capacity of DNA melting from temperature dependence of single molecule stretching. Biophys J 80(4):1932–1939
292. Bustamante C, Smith SB, Liphardt J, Smith D (2000) Single-molecule studies of DNA mechanics. Curr Opin Struct Biol 10(3):279–285
293. Baumann CG, Smith SB, Bloomfield VA, Bustamante C (1997) Ionic effects on the elasticity of single DNA molecules. Proc Natl Acad Sci 94(12):6185–6190
294. Wang MD, Yin H, Landick R, Gelles J, Block SM (1997) Stretching DNA with optical tweezers. Biophys J 72(3):1335–1346
295. Wenner JR, Williams MC, Rouzina I, Bloomfield VA (2002) Salt dependence of the elasticity and overstretching transition of single DNA molecules. Biophys J 82(6):3160
296. Chiou C-H, Huang Y-Y, Chiang M-H, Lee H-H, Lee G-B (2006) New magnetic tweezers for investigation of the mechanical properties of single DNA molecules. Nanotechnology 17(5):1217
297. Goodman RP, Schaap IA, Tardin CF, Erben CM, Berry RM, Schmidt CF, Turberfield AJ (2005) Rapid chiral assembly of rigid DNA building blocks for molecular nanofabrication. Science 310(5754):1661–1665
298. Morii T, Mizuno R, Haruta H, Okada T (2004) An AFM study of the elasticity of DNA molecules. Thin Solid Films 464:456–458
299. Vafabakhsh R, Ha T (2012) Extreme bendability of DNA less than 100 base pairs long revealed by single-molecule cyclization. Science 337(6098):1097–1101
300. Ke C, Humeniuk M, S-Gracz H, Marszalek PE (2007) Direct measurements of base stacking interactions in DNA by single-molecule atomic-force spectroscopy. Phys Rev Lett 99(1):018302–018304
301. W-s C, Chen W-H, Chen Z, Gooding AA, Lin K-J, Kiang C-H (2010) Direct observation of multiple pathways of single-stranded DNA stretching. Phys Rev Lett 105(21):218104
302. Ke C, Loksztejn A, Jiang Y, Kim M, Humeniuk M, Rabbi M, Marszalek PE (2009) Detecting solvent-driven transitions of poly (A) to double-stranded conformations by atomic force microscopy. Biophys J 96(7):2918–2925
303. Seol Y, Skinner GM, Visscher K, Buhot A, Halperin A (2007) Stretching of homopolymeric RNA reveals single-stranded helices and base-stacking. Phys Rev Lett 98(15):158103
304. Rief M, Clausen-Schaumann H, Gaub HE (1999) Sequence-dependent mechanics of single DNA molecules. Nat Struct Mol Biol 6(4):346–349
305. Clausen-Schaumann H, Rief M, Tolksdorf C, Gaub HE (2000) Mechanical stability of single DNA molecules. Biophys J 78(4):1997–2007
306. Lee G, Rabbi M, Clark RL, Marszalek PE (2007) Nanomechanical fingerprints of UV damage to DNA. Small 3(5):809–813
307. Saenger W (1984) Principles of nucleic acid structure, vol 7. Springer-Verlag, New York
308. Marszalek PE, Pang YP, Li HB, El Yazal J, Oberhauser AF, Fernandez JM (1999) Atomic levers control pyranose ring conformations. Proc Natl Acad Sci USA 96(14):7894–7898
309. Zhang QM, Lee GR, Marszalek PE (2005) Atomic cranks and levers control sugar ring conformations. J Phys Condens Matter 17(18):S1427–S1442
310. Zhang QM, Marszalek PE (2006) Solvent effects on the elasticity of polysaccharide molecules in disordered and ordered states by single-molecule force spectroscopy. Polymer 47(7):2526–2532

311. Li HB, Rief M, Oesterhelt F, Gaub HE, Zhang X, Shen JC (1999) Single-molecule force spectroscopy on polysaccharides by AFM – nanomechanical fingerprint of alpha-(1,4)-linked polysaccharides. Chem Phys Lett 305(3–4):197–201
312. Lee W, Zeng X, Yang W, Marszalek PE (2012) Mechanics of polysaccharides. In: Anne-Sophie Duwez NW (ed) Molecular manipulation with atomic force microscopy. CRC Press, Boca Raton/London/New York
313. Lee G, Nowak W, Jaroniec J, Zhang Q, Marszalek PE (2004) Nanomechanical control of glucopyranose rotamers. J Am Chem Soc 126(20):6218–6219
314. Lee G, Nowak W, Jaroniec J, Zhang Q, Marszalek PE (2004), Molecular dynamics simulations of forced conformational transitions in 1,6-linked polysaccharides. Biophys J, 87(3):1456–1465.
315. Li H, Rief M, Oesterhelt F, Gaub HE (1999) Force spectroscopy on single xanthan molecules. Appl Phys A-Mater Sci Process 68(4):407–410
316. Li HB, Rief M, Oesterhelt F, Gaub HE (1998) Single-molecule force spectroscopy on Xanthan by AFM. Adv Mater 10(4):316–319
317. Marszalek PE, Li HB, Fernandez JM (2001) Fingerprinting polysaccharides with single-molecule atomic force microscopy. Nat Biotechnol 19(3):258–262
318. Marszalek PE, Li HB, Oberhauser AF, Fernandez JM (2002) Chair-boat transitions in single polysaccharide molecules observed with force-ramp AFM. Proc Natl Acad Sci USA 99(7):4278–4283
319. Zhang Q, Jaroniec J, Lee G, Marszalek PE (2005) Direct detection of inter-residue hydrogen bonds in polysaccharides by single-molecule force spectroscopy. Angew Chem Int Ed 44(18):2723–2727
320. Zhang Q, Lu Z, Hu H, Yang W, Marszalek PE (2006) Direct detection of the formation of V-Amylose helix by single molecule force spectroscopy. J Am Chem Soc 128(29):9387–9393
321. Zhang Q, Marszalek PE (2006) Solvent effects on the elasticity of polysaccharide molecules in disordered and ordered states by single-molecule force spectroscopy. Polymer 47(7):2526–2532
322. Lu ZY, Nowak W, Lee GR, Marszalek PE, Yang WT (2004) Elastic properties of single amylose chains in water: a quantum mechanical and AFM study. J Am Chem Soc 126(29):9033–9041
323. Lee G, Nowak W, Jaroniec J, Zhang Q, Marszalek PE (2004) Molecular dynamics simulations of forced conformational transitions in 1,6-linked polysaccharides. Biophys J 87(3):1456–1465
324. Zhang QM, Marszalek PE (2006) Identification of sugar isomers by single-molecule force spectroscopy. J Am Chem Soc 128(17):5596–5597
325. Xu Q, Zhang W, Zhang X (2002) Oxygen bridge inhibits conformational transition of 1,4-linked -galactose detected by single-molecule atomic force microscopy. Macromolecules 35(3):871–876
326. Marszalek PE, Oberhauser AF, Li HB, Fernandez JM (2003) The force-driven conformations of heparin studied with single molecule force microscopy. Biophys J 85(4):2696–2704
327. Zhang L, Wang C, Cui S, Wang Z, Zhang X (2003) Single-molecule force spectroscopy on curdlan: unwinding helical structures and random coils. Nano Lett 3(8):1119–1124. doi:10.1021/nl034298d
328. Struckmeier J, Wahl R, Leuschner M, Nunes J, Janovjak H, Geisler U, Hofmann G, Jähnke T, Müller DJ (2008) Fully automated single-molecule force spectroscopy for screening applications. Nanotechnology 19(38):384020
329. Churnside AB, Sullan RMA, Nguyen DM, Case SO, Bull MS, King GM, Perkins TT (2012) Routine and timely sub-picoNewton force stability and precision for biological applications of atomic force microscopy. Nano Lett 12(7):3557–3561